# CHAPTER 3

## Results

### 3.1 Raw material characteristics

Trace elements concentrations of $CaCO_3$ were found to contain arsenic (AS) below 0.32 ppm and cadmium (Cd) below 0.01 ppm. Mercury (Hg) and Lead (Pb) were not detectable in $CaCO_3$. Total heavy metals had less than 50 ppm. In **Figure 12,** XRD pattern of the $CaCO_3$ powders were presented. The Result of this study revealed contained phase of calcite (JCPDS file no. 85-1108) which was pure $CaCO_3$.

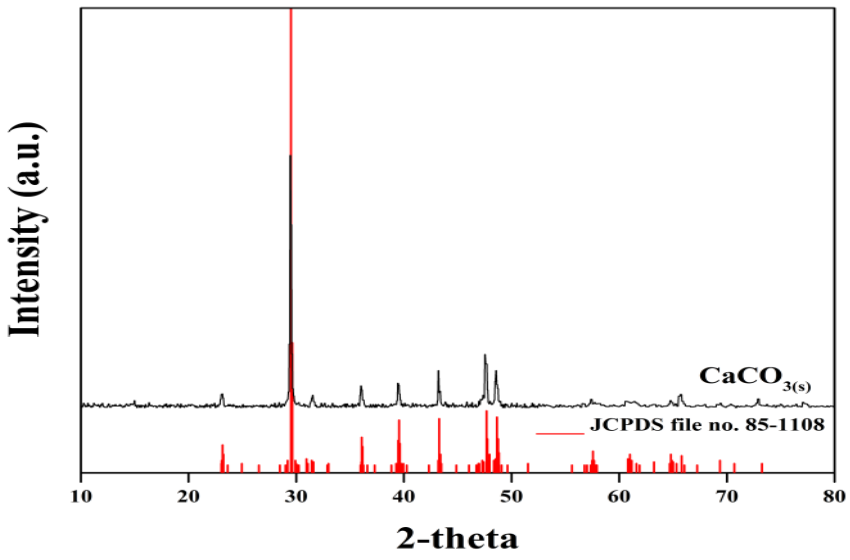




**Figure 12** XRD pattern of the $CaCO_3$ powders at 650 °C 5 hours

It was found that the particle size distribution of mixed powder before and after milling was differences as shown in **Figure 12**.

**Figure 13** shows powder mixtures before milling, particle size distribution was not homogenous and can be divided into two groups of particles populations (curve (a), while, after milling, partly homogenous and are separated into three groups (curve (b) due to different sizes of starting materials and insufficiency of mechanical energy. The average particle size was approximately 11.04 ± 0.06 μm. The size distribution of ground powders were between 0.3 and 14 μm. The specific surface area was 3.7228 ± 0.01 $m^2/g$. These values would be appropriate for forming the ceramic bodies and sintering at high temperature.

The mixed powder consists of irregular shapes agglomerates probably due to electrostatic and van der Waal's attraction between particles or liquid capillary forces as a result of the presence of reaching the melting point of $NH_4H_2PO_4$ (190°C) during milling process.

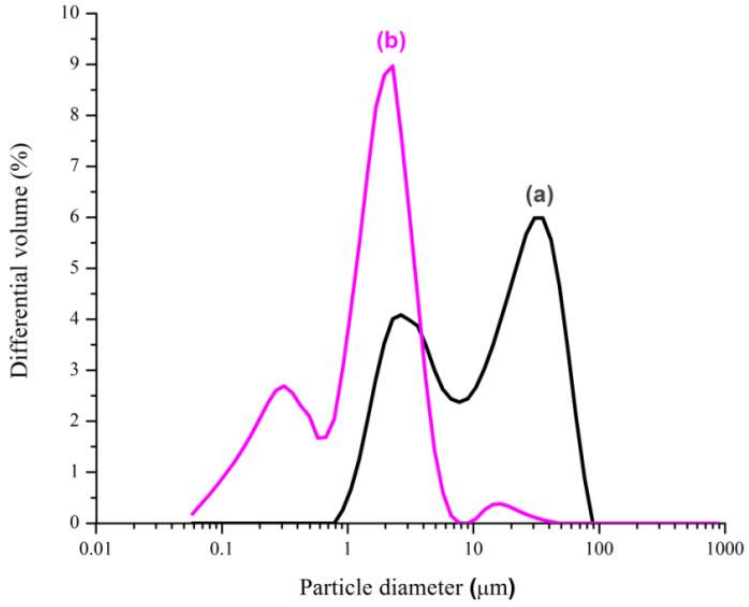


**Figure 13** Particle size distribution of mixed powder (a) before milling (b) after milling.

## 3.2 Physical properties of mixed powder

### Thermal analysis

Thermal analysis was physical property of material for to know materials reactivity under sintering temperature. The TG showed the weight loss of sample powder. This result could be divided the seventh stages in **Table 3**. The thermogram of mixed powder showed continuously endothermic and exothermic evolution and three distinct thermal events during the reaction of $CaCO_3$ and $NH_4H_2PO_4$. The composition of precursors could formed as HA in **Table 4**.

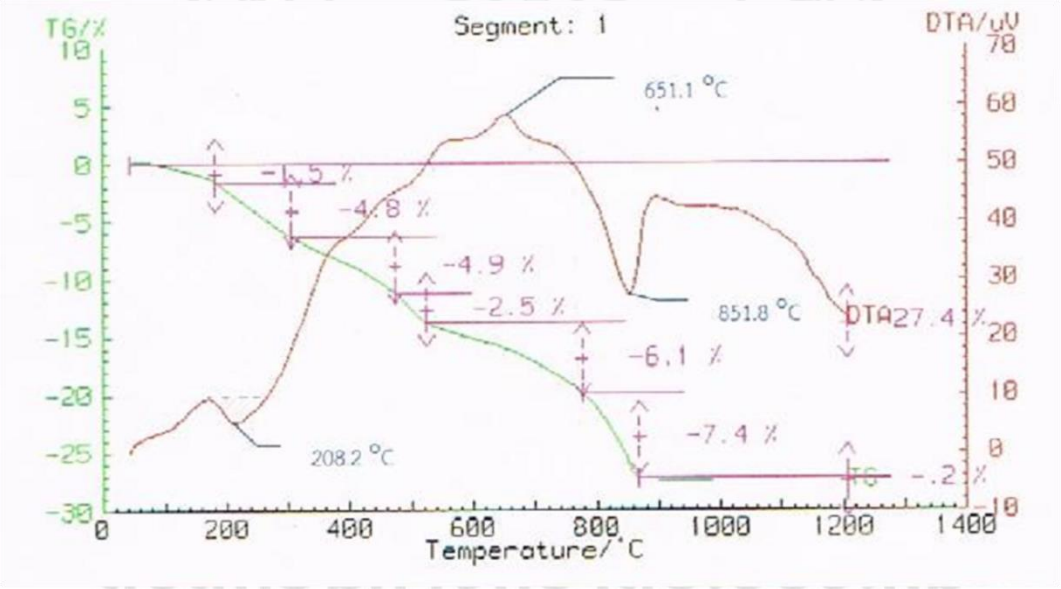




**Figure 14** DTA/TG analyses curves of mixed powder with Ca/P ratio of 1.67

In **Figure 14,** solid state reaction used thermal analysis for studying reaction between $CaCO_3$ and $NH_4H_2PO_4$ powders. Mixed powder was ratio of Ca/P 1.67 for the formation of single phase HA. The first endothermic peak was range from 182.2 to 305.5 °C. This reaction was losing weight of ammonia and water vapor about 4.8 %.

The second exothermic peak took place between 523.4 and 775.5 °C, which shown in this curve occurred the phase transition from amorphous $Ca_2P_2O_7$ ($\gamma$-$Ca_2P_2O_7$) to beta-$Ca_2P_2O_7$ and possible to decomposition of $CaCO_3$ into CaO, which weight loss was about 6.1 %. The third endothermic peak was range from 775.5 to 867.7 °C. This reaction caused by remain of $CaCO_3$ and transform to CaO occurred $CO_2$ gas released in lose weight about 7.4 wt%. This reaction started formation of β-TCP, HA, β-$Ca_2P_2O_7$ phase and remained of CaO.

**Table 3** Results of lose weight.

| TG | |
|---|---|
| Temperature range of weight loss (°C) | Lose weight (%) |
| 43.5-182.2 | 1.5 |
| 182.2-305.5 | 4.8 |
| 305.5-473.2 | 4.9 |
| 473.2-523.4 | 2.5 |
| 523.4-775.5 | 6.1 |
| 775.5-867.7 | 7.4 |
| 867.7-1205.4 | 0.2 |
| Total lose weight | 27.4 |

**Table 4** Results of reaction.

| DTA | |
|---|---|
| Type of reaction | Temperature (°C) |
| Endothermic | 208.2 |
| Exothermic | 651.1 |
| Endothermic | 851.8 |



The observed total weight loss was 27.4 % from ambient temperature to 1200 °C. **Table 3** and **4** were summarized the above results could be explained that three distinct thermal events during the reaction of $CaCO_3$ and $NH_4H_2PO_4$. The solid state reaction between both materials mixed with Ca/P mole ratio of 1.67 to form HA.

The detailed solid state reaction sequence between the starting powders upon heating might be concluded as follows:

$$CaCO_{3(s)} + NH_4H_2PO_{4(s)} \xrightarrow{\sim 44 - 182^{\circ}C} CaCO_{3(s)} + NH_4OH_{(l)} + H_3PO_{4(l)} \quad [82]$$

$$CaCO_{3(s)} + 2NH_4H_2PO_{4(l)} \xrightarrow{\sim 182 - 305^{\circ}C} P_2O_{5(s)} + CaCO_{3(s)} + 2NH_{3(g)} + 3H_2O_{(g)} \quad [88]$$

$$4CaCO_{3(s)} + P_2O_{5(s)} \xrightarrow{\sim 305 - 473^{\circ}C} \gamma\text{-}Ca_2P_2O_{7(s)} + 2CaCO_{3(s)} + 4CO_{2(g)} \quad [88]$$

$$\gamma\text{-}Ca_2P_2O_{7(s)} + 2CaCO_{3(s)} \xrightarrow{\sim 473 - 523^{\circ}C} \gamma\text{-}Ca_2P_2O_{7(s)} + CaCO_{3(s)} + CaO_{(s)} + CO_{2(g)} \quad [88]$$

$$\gamma\text{-}Ca_2P_2O_{7\,(s)} + 2CaCO_{3(s)} \xrightarrow{\sim 523 - 775^{\circ}C} \beta\text{-}Ca_2P_2O_{7(s)} + CaCO_{3(s)} + 2CaO_{(s)} + CO_{2(g)} + CaO_{(s)} \quad [17, 72]$$

$$\beta\text{-}Ca_2P_2O_{7(s)} + CaCO_{3(s)} \xrightarrow{\sim 775 - 867^{\circ}C} \beta\text{-}Ca_2P_2O_{7(s)} + Ca_{10}(PO_4)_6(OH)_{2(s)} + CaO_{(s)} + CaO_{(s)} + \beta\text{-}Ca_3(PO_4)_{2(s)} + CO_{2(g)} \quad [17, 72]$$

$$\beta\text{-}Ca_3(PO_4)_{2(s)} + CaO_{(s)} \xrightarrow{\sim 867 - 1205^{\circ}C} \beta\text{-}Ca_3(PO_4)_{2(s)} + Ca_{10}(PO_4)_6(OH)_{2-2x}O_xV_{(s)} + Ca_{10}(PO_4)_6(OH)_{2(s)} + \beta\text{-}Ca_2P_2O_{7(s)} + CaO_{(s)}\ ;\ \text{if } x = 1 \quad [17, 72]$$

$$Ca_{10}(PO_4)_6O_{(s)} + Ca_3(PO_4)_{2(s)} + CaO_{(s)} \xrightarrow{\sim 1205 - 1300^{\circ}C} Ca_{10}(PO_4)_6O_{(s)} + Ca_3(PO_4)_{2(s)} + CaO_{(s)} \quad [17, 72]$$

$$Ca_{10}(PO_4)_6O_{(s)} + Ca_3(PO_4)_{2(s)} + CaO_{(s)} \xrightarrow{\text{rehydrate OH}} Ca_{10}(PO_4)_6(OH)_{2(s)} + Ca_3(PO_4)_{2(s)} + CaO_{(s)} \quad [17, 72]$$

When the temperature was range from 775 to 867 °C, HA phase seem gradually increased while β-TCP had high quantity. At the temperatures range from 867 to 1205 °C, HA was dehydrated into oxyhydroxyapatite (OHA) ($Ca_{10}(PO_4)_6(OH)_{2-2x}O_xV$) and expected when the temperature at 1100, 1150 and 1205

°C. OHA, where x = 1 and V was lattice vacancy in the $OH^-$ position along the crystallographic. Then, OHA was transformed to oxyapatite $Ca_{10}(PO_4)_6OV$ or $Ca_{10}(PO_4)_6O$. This study could be explained that the formation of β-TCP was faster than of HA, but HA was more thermodynamically stable than β-TCP. Hence, the formed β-TCP was continually reaction with CaO, which could also be detected below 867 °C by XRD technique and when the temperature was increased up to 1250 °C and 1300 °C, both β-TCP and CaO remained be impurities phases and then oxyapatite could be rehydroxylation by annealing route and cool down to room temperature from firing profile of sintering schedule which transforms into HA and β-TCP and CaO. Finally, the rehydroxylation of oxyapatite to HA while remained phase showed both β-TCP and CaO phases due to incomplete process of cooling modes [17].

### 3.3 Physical properties of sintered samples

#### Density and porosity measurements

**Table 5** showed densities and porosities of samples with various Ca/P ratios 1.65, 1.66, 1.67, 1.68 and 1.69 at 1100, 1150, 1200, 1250 and 1300 °C for 2, 3, 4 and 5 hours. The result was derived from an average of six samples for each condition of sintering temperatures, compositions and soaking times.

**Table 5** Effect of sintering temperature on density and apparent porosity.

| Sample | Apparent density ($g/cm^3$) | Bulk density ($g/cm^3$) | True density ($g/cm^3$) | Apparent porosity (%) |
|---|---|---|---|---|
| 1A-2 | 2.80 ± 0.02 | 1.21 ± 0.01 | 2.817 ± 0.001 | 56.82 ± 0.70 |
| 1B-2 | 2.82 ± 0.05 | 1.22 ± 0.02 | 2.833 ± 0.003 | 56.61 ± 0.31 |
| 1C-2 | 2.89 ± 0.02 | 1.38 ± 0.02 | 2.902 ± 0.009 | 52.18 ± 0.35 |
| 1D-2 | 2.97 ± 0.02 | 1.45 ± 0.02 | 3.016 ± 0.003 | 51.35 ± 0.38 |
| 1E-2 | 3.04 ± 0.03 | 1.49 ± 0.01 | 3.067 ± 0.002 | 51.20 ± 0.34 |
| 1A-3 | 2.67 ± 0.06 | 1.19 ± 0.02 | 2.686 ± 0.002 | 55.60 ± 0.38 |
| 1B-3 | 2.73 ± 0.01 | 1.28 ± 0.01 | 2.745 ± 0.001 | 53.04 ± 0.46 |
| 1C-3 | 2.91 ± 0.01 | 1.37 ± 0.01 | 2.918 ± 0.002 | 52.98 ± 0.44 |
| 1D-3 | 2.99 ± 0.03 | 1.49 ± 0.01 | 3.027 ± 0.001 | 50.20 ± 0.52 |
| 1E-3 | 2.99 ± 0.03 | 1.47 ± 0.01 | 3.095 ± 0.002 | 50.79 ± 0.43 |
| 1A-4 | 2.72 ± 0.04 | 1.19 ± 0.01 | 2.749 ± 0.001 | 56.11 ± 0.85 |
| 1B-4 | 2.86 ± 0.03 | 1.31 ± 0.02 | 2.866 ± 0.001 | 54.15 ± 0.43 |
| 1C-4 | 2.89 ± 0.05 | 1.36 ± 0.02 | 2.897 ± 0.001 | 52.88 ± 0.30 |
| 1D-4 | 2.96 ± 0.03 | 1.48 ± 0.02 | 2.987 ± 0.002 | 49.97 ± 0.48 |
| 1E-4 | 2.96 ± 0.04 | 1.45 ± 0.03 | 3.061 ± 0.002 | 51.12 ± 0.32 |

**Table 5** (Cont'd)

| Sample | Apparent density ($g/cm^3$) | Bulk density ($g/cm^3$) | True density ($g/cm^3$) | Apparent porosity (%) |
|---|---|---|---|---|
| 1A-5 | 2.78 ± 0.03 | 1.20 ± 0.01 | 2.799 ± 0.005 | 56.78 ± 0.31 |
| 1B-5 | 2.82 ± 0.03 | 1.28 ± 0.02 | 2.848 ± 0.001 | 54.75 ± 0.36 |
| 1C-5 | 2.91 ± 0.03 | 1.39 ± 0.02 | 2.923 ± 0.001 | 52.34 ± 0.32 |
| 1D-5 | 2.95 ± 0.03 | 1.50 ± 0.03 | 2.970 ± 0.002 | 49.14 ± 0.68 |
| 1E-5 | 3.00 ± 0.03 | 1.53 ± 0.01 | 3.043 ± 0.001 | 48.98 ± 0.64 |
| 2A-2 | 2.82 ± 0.05 | 1.22 ± 0.01 | 2.818 ± 0.001 | 56.50 ± 0.84 |
| 2B-2 | 2.84 ± 0.04 | 1.24 ± 0.01 | 2.844 ± 0.002 | 56.10 ± 0.54 |
| 2C-2 | 2.94 ± 0.02 | 1.42 ± 0.01 | 2.967 ± 0.002 | 51.86 ± 0.29 |
| 2D-2 | 2.99 ± 0.04 | 1.48 ± 0.01 | 3.023 ± 0.002 | 50.40 ± 0.43 |
| 2E-2 | 3.05 ± 0.03 | 1.54 ± 0.02 | 3.071 ± 0.002 | 49.38 ± 0.83 |
| 2A-3 | 2.74 ± 0.04 | 1.22 ± 0.01 | 2.766 ± 0.001 | 55.36 ± 0.76 |
| 2B-3 | 2.79 ± 0.02 | 1.32 ± 0.01 | 2.807 ± 0.002 | 52.64 ± 0.53 |
| 2C-3 | 2.91 ± 0.03 | 1.38 ± 0.01 | 2.944 ± 0.002 | 52.53 ± 0.21 |
| 2D-3 | 3.04 ± 0.03 | 1.60 ± 0.02 | 3.043 ± 0.005 | 47.15 ± 0.45 |
| 2E-3 | 3.03 ± 0.03 | 1.57 ± 0.02 | 3.097 ± 0.002 | 48.30 ± 0.46 |
| 2A-4 | 2.80 ± 0.04 | 1.24 ± 0.02 | 2.806 ± 0.001 | 55.92 ± 0.17 |
| 2B-4 | 2.87 ± 0.01 | 1.34 ± 0.01 | 2.890 ± 0.001 | 53.55 ± 0.08 |
| 2C-4 | 2.91 ± 0.03 | 1.41 ± 0.03 | 2.907 ± 0.002 | 51.65 ± 0.57 |
| 2D-4 | 2.98 ± 0.03 | 1.53± 0.02 | 2.995 ± 0.003 | 48.55 ± 0.42 |
| 2E-4 | 2.96 ± 0.01 | 1.51 ± 0.02 | 3.065 ± 0.001 | 48.99 ± 0.62 |
| 2A-5 | 2.86 ± 0.03 | 1.24 ± 0.01 | 2.869 ± 0.003 | 56.53 ± 0.80 |
| 2B-5 | 2.92 ± 0.02 | 1.36 ± 0.02 | 2.940 ± 0.002 | 53.57 ± 0.33 |
| 2C-5 | 2.94 ± 0.05 | 1.41 ± 0.02 | 2.954 ± 0.003 | 52.05 ± 0.54 |

**Table 5** (Cont'd)

| Sample | Apparent density ($g/cm^3$) | Bulk density ($g/cm^3$) | True density ($g/cm^3$) | Apparent porosity (%) |
|---|---|---|---|---|
| 2D-5 | 3.01 ± 0.03 | 1.56 ± 0.03 | 3.028 ± 0.001 | 48.35 ± 0.74 |
| 2E-5 | 3.03 ± 0.03 | 1.57 ± 0.01 | 3.079 ± 0.003 | 48.13 ± 0.76 |
| 3A-2 | 2.82 ± 0.10 | 1.24 ± 0.02 | 2.820 ± 0.003 | 55.81 ± 1.84 |
| 3B-2 | 2.86 ± 0.05 | 1.26 ± 0.01 | 2.860 ± 0.001 | 55.66 ± 0.62 |
| 3C-2 | 2.95 ± 0.03 | 1.44 ± 0.01 | 2.971 ± 0.001 | 51.31 ± 0.35 |
| 3D-2 | 3.00 ± 0.03 | 1.51 ± 0.02 | 3.029 ± 0.002 | 49.57 ± 0.44 |
| 3E-2 | 3.08 ± 0.03 | 1.78 ± 0.02 | 3.092 ± 0.001 | 42.39 ± 0.36 |
| 3A-3 | 2.77 ± 0.05 | 1.24 ± 0.01 | 2.776 ± 0.001 | 55.06 ± 0.76 |
| 3B-3 | 2.79 ± 0.05 | 1.34 ± 0.01 | 2.811 ± 0.001 | 52.19 ± 0.52 |
| 3C-3 | 2.94 ± 0.04 | 1.41 ± 0.02 | 2.967 ± 0.002 | 51.94 ± 0.61 |
| 3D-3 | 3.05 ± 0.04 | 1.91 ± 0.03 | 3.060 ± 0.001 | 37.33 ± 0.50 |
| 3E-3 | 3.03 ± 0.06 | 1.61 ± 0.04 | 3.112 ± 0.002 | 46.93 ± 1.04 |
| 3A-4 | 2.86 ± 0.03 | 1.29 ± 0.01 | 2.867 ± 0.002 | 54.90 ± 0.50 |
| 3B-4 | 2.88 ± 0.03 | 1.38 ± 0.01 | 2.909 ± 0.001 | 52.22 ± 0.50 |
| 3C-4 | 2.94 ± 0.03 | 1.43 ± 0.01 | 2.983 ± 0.002 | 51.39 ± 0.22 |
| 3D-4 | 3.01 ± 0.04 | 1.96 ± 0.03 | 3.018 ± 0.001 | 35.05 ± 0.24 |
| 3E-4 | 2.99 ± 0.03 | 1.62 ± 0.02 | 3.084 ± 0.001 | 45.70 ± 0.72 |
| 3A-5 | 2.90 ± 0.03 | 1.28 ± 0.01 | 2.907 ± 0.002 | 55.85 ± 0.52 |
| 3B-5 | 2.93 ± 0.03 | 1.39 ± 0.01 | 2.951 ± 0.002 | 52.65 ± 0.35 |
| 3C-5 | 2.96 ± 0.02 | 1.44 ± 0.02 | 2.980 ± 0.002 | 51.28 ± 0.53 |
| 3D-5 | 3.02 ± 0.02 | 1.99 ± 0.04 | 3.068 ± 0.002 | 34.15 ± 1.06 |
| 3E-5 | 3.01 ± 0.04 | 1.62 ± 0.03 | 3.088 ± 0.003 | 46.09 ± 0.37 |
| 4A-2 | 2.85 ± 0.05 | 1.26 ± 0.02 | 2.882 ± 0.004 | 55.67 ± 1.14 |

**Table 5** (Cont'd)

| Sample | Apparent density ($g/cm^3$) | Bulk density ($g/cm^3$) | True density ($g/cm^3$) | Apparent porosity (%) |
|---|---|---|---|---|
| 4B-2 | 2.92 ± 0.03 | 1.34 ± 0.01 | 2.922 ± 0.001 | 54.16 ± 0.41 |
| 4C-2 | 2.96 ± 0.04 | 1.46 ± 0.02 | 2.977 ± 0.002 | 50.81 ± 0.65 |
| 4D-2 | 3.00 ± 0.04 | 1.56 ± 0.02 | 3.046 ± 0.014 | 48.09 ± 0.48 |
| 4E-2 | 3.14 ± 0.04 | 2.29 ± 0.04 | 3.142 ± 0.003 | 26.97 ± 0.58 |
| 4A-3 | 2.80 ± 0.02 | 1.27 ± 0.01 | 2.818 ± 0.002 | 54.64 ± 0.23 |
| 4B-3 | 2.87 ± 0.02 | 1.38 ± 0.02 | 2.900 ± 0.001 | 52.07 ± 0.88 |
| 4C-3 | 2.96 ± 0.03 | 1.45 ± 0.02 | 2.996 ± 0.003 | 50.81 ± 0.56 |
| 4D-3 | 3.06 ± 0.04 | 1.97 ± 0.04 | 3.074 ± 0.003 | 35.72 ± 0.42 |
| 4E-3 | 3.04 ± 0.05 | 1.67 ± 0.02 | 3.123 ± 0.002 | 45.20 ± 0.72 |
| 4A-4 | 2.87 ± 0.03 | 1.33 ± 0.02 | 2.896 ± 0.002 | 53.83 ± 0.36 |
| 4B-4 | 2.93 ± 0.01 | 1.42 ± 0.01 | 2.941 ± 0.002 | 51.68 ± 0.28 |
| 4C-4 | 2.99 ± 0.02 | 1.48 ± 0.02 | 3.013 ± 0.001 | 50.59 ± 0.76 |
| 4D-4 | 3.03 ± 0.05 | 2.05 ± 0.03 | 3.056 ± 0.001 | 32.39 ± 0.36 |
| 4E-4 | 3.01 ± 0.03 | 1.69 ± 0.03 | 3.109 ± 0.003 | 43.98 ± 0.85 |
| 4A-5 | 2.90 ± 0.04 | 1.34 ± 0.02 | 2.922 ± 0.002 | 53.96 ± 0.53 |
| 4B-5 | 2.94 ± 0.03 | 1.41 ± 0.01 | 2.957 ± 0.002 | 52.06 ± 0.58 |
| 4C-5 | 2.96 ± 0.02 | 1.46 ± 0.01 | 2.986 ± 0.003 | 50.80 ± 0.28 |
| 4D-5 | 3.04 ± 0.03 | 2.10 ± 0.02 | 3.071 ± 0.003 | 31.10 ± 0.45 |
| 4E-5 | 3.02 ± 0.02 | 1.70 ± 0.02 | 3.092 ± 0.003 | 43.65 ± 0.69 |
| 5A-2 | 2.88 ± 0.02 | 1.29 ± 0.01 | 2.887 ± 0.002 | 55.27 ± 0.38 |
| 5B-2 | 2.93 ± 0.02 | 1.36 ± 0.01 | 2.953 ± 0.001 | 53.54 ± 0.48 |
| 5C-2 | 2.98 ± 0.02 | 1.52 ± 0.01 | 2.998 ± 0.002 | 49.03 ± 0.21 |
| 5D-2 | 3.05 ± 0.04 | 2.14 ± 0.03 | 3.141 ± 0.003 | 30.05 ± 0.42 |

**Table 5** (Cont'd)

| Sample | Apparent density ($g/cm^3$) | Bulk density ($g/cm^3$) | True density ($g/cm^3$) | Apparent porosity (%) |
|---|---|---|---|---|
| 5E-2 | 3.14 ± 0.03 | 2.38 ± 0.03 | 3.145 ± 0.002 | 24.37 ± 0.51 |
| 5A-3 | 2.84 ± 0.05 | 1.31 ± 0.03 | 2.862 ± 0.002 | 53.81 ± 0.40 |
| 5B-3 | 2.93 ± 0.02 | 1.42 ± 0.01 | 2.998 ± 0.001 | 51.54 ± 0.22 |
| 5C-3 | 2.97 ± 0.04 | 1.50 ± 0.02 | 3.021 ± 0.002 | 49.57 ± 0.43 |
| 5D-3 | 3.09 ± 0.02 | 2.01 ± 0.01 | 3.114 ± 0.002 | 35.11 ± 0.26 |
| 5E-3 | 3.08 ± 0.03 | 1.80 ± 0.02 | 3.141 ± 0.001 | 41.34 ± 0.57 |
| 5A-4 | 2.88 ± 0.05 | 1.35 ± 0.02 | 2.904 ± 0.003 | 52.88 ± 0.30 |
| 5B-4 | 2.94 ± 0.02 | 1.45 ± 0.02 | 2.960 ± 0.001 | 50.69 ± 0.53 |
| 5C-4 | 3.02 ± 0.02 | 1.54 ± 0.01 | 3.018 ± 0.002 | 49.00 ± 0.42 |
| 5D-4 | 3.04 ± 0.03 | 2.07 ± 0.03 | 3.102 ± 0.002 | 31.87 ± 0.73 |
| 5E-4 | 3.03 ± 0.02 | 1.94 ± 0.02 | 3.124 ± 0.002 | 35.91 ± 0.83 |
| 5A-5 | 2.90 ± 0.07 | 1.37 ± 0.03 | 2.927 ± 0.002 | 52.87 ± 0.28 |
| 5B-5 | 2.95 ± 0.07 | 1.44 ± 0.01 | 2.958 ± 0.001 | 51.14 ± 1.28 |
| 5C-5 | 3.04 ± 0.03 | 1.57 ± 0.01 | 3.049 ± 0.002 | 48.17 ± 0.30 |
| 5D-5 | 3.07 ± 0.04 | 2.19 ± 0.04 | 3.073 ± 0.002 | 28.54 ± 0.45 |
| 5E-5 | 3.03 ± 0.01 | 2.10 ± 0.02 | 3.104 ± 0.002 | 30.72 ± 0.41 |

**Note:** 1, 2, 3, 4, 5 (front) = 1.65, 1.66, 1.67, 1.68, 169
A, B, C, D, E = 1100 °C, 1150 °C, 1200 °C, 1250 °C, 1300 °C
2, 3, 4, 5 (behind) = 2 hours, 3 hours, 4 hours, 5 hours

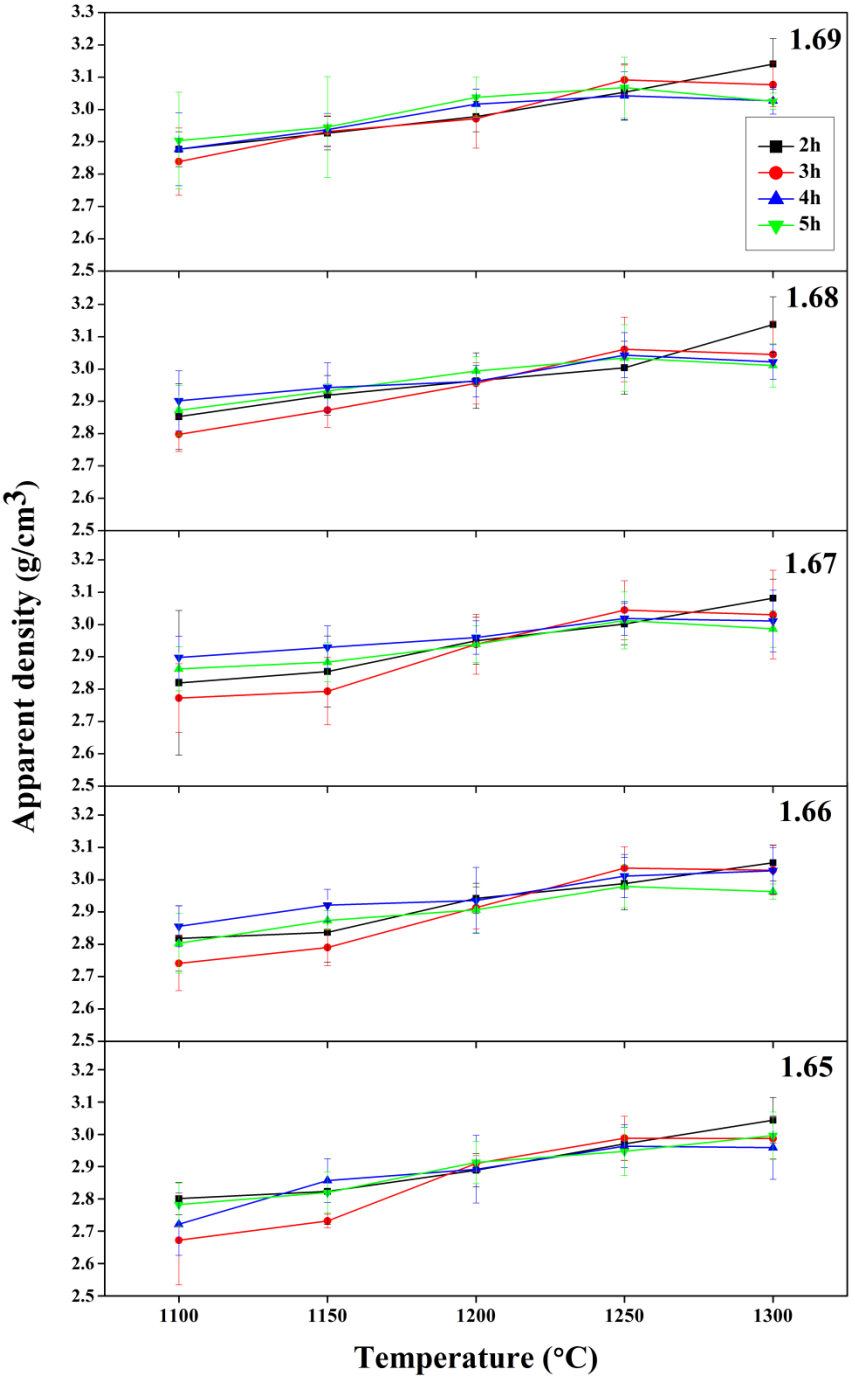


**Figure 15** Apparent densities of Ca/P ratios 1.65, 1.66, 1.67, 1.68 and 1.69 at different temperatures and times.

**Figure 15** showed curves of the apparent density variation as a function of sintering temperatures. This density included the solid component and closed pores. The overall trend of these curves showed behavior increased densities with increased sintering temperatures. These curves indicated that densification process of each grain boundary start at 1100 °C to the maximum apparent densities at 1250 °C for 3 and 4 hours with samples Ca/P ratio of 1.65, 1.66, 1.67, 1.68 and 1.69. In addition, for 5 hours with samples Ca/P ratios of 1.67, 1.68 and 1.69 showed the maximum apparent densities was same. However, the samples sintered at 1300 °C with Ca/P ratios of 1.65, 1.66, 1.67, 1.68 and 1.69 for 2 hours indicated maximum apparent densities and the samples Ca/P ratios of 1.65 and 1.66 showed the maximum apparent densities for 5 hours was same. The maximum apparent densities of all condition when compared with the same temperature showed that a sintering at 1300 °C for 2 hours with samples ratio 1.69 was $3.14 \pm 0.03$ g/cm$^3$, which closed to the theoretical density of pure HA 3.16 g/cm$^3$.

This behavior could be explained that at high sintering temperature, the densification rate had high and the compacts sample exhibited moderate to high grain growth. Any difference in initial particle sizes led to driving forces on the grain boundaries that caused grain growth, when the temperature was increased, then the rate of grain boundary activation increases and might be breakaway of the boundaries from many pores in microstructure and leaving of isolated pores in the internal grain.

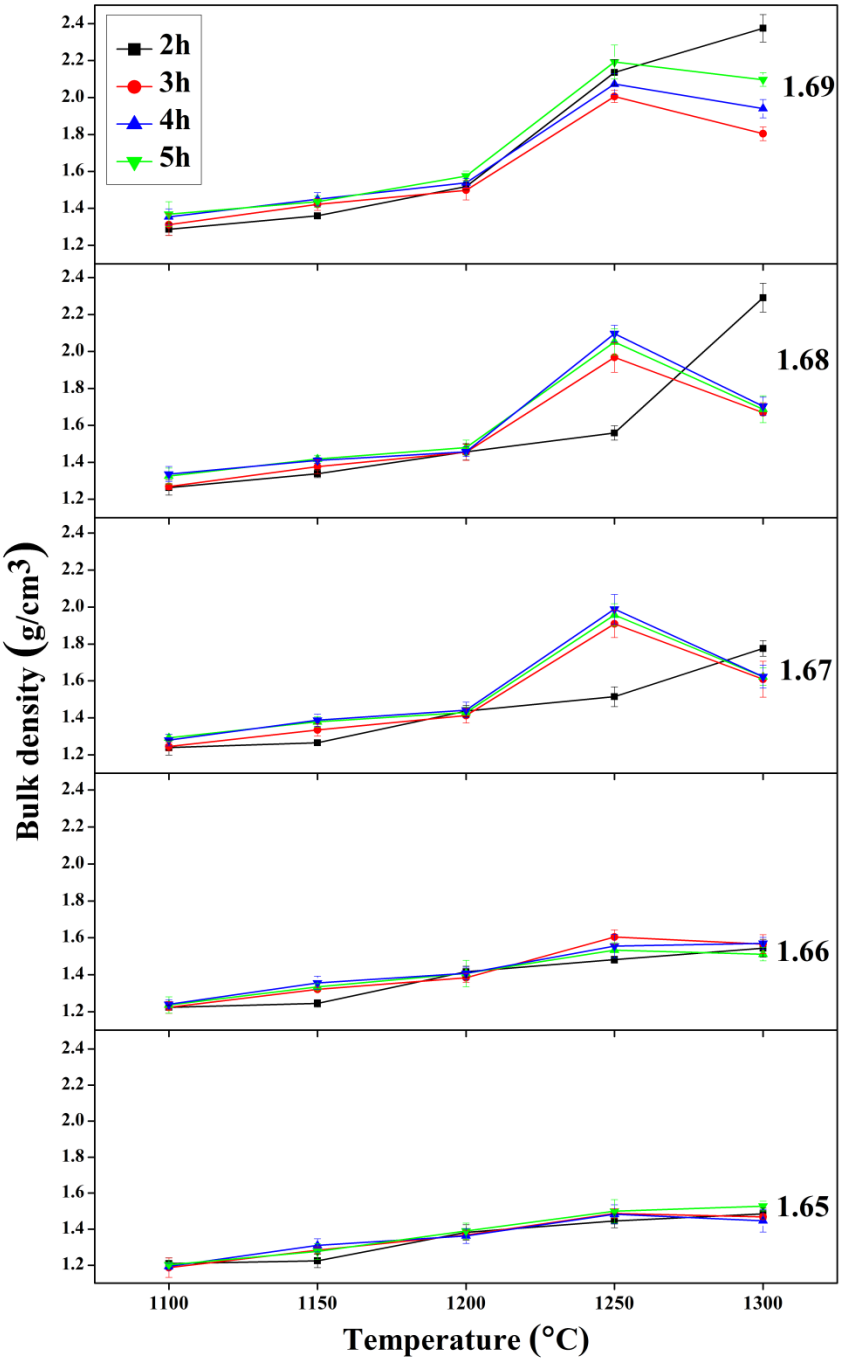


**Figure 16** Bulk densities of Ca/P ratios 1.65, 1.66, 1.67, 1.68 and 1.69 at different temperatures and times.

**Figure 16** showed curves of the bulk density variation as a function of sintering temperatures. This density included the solid component, opened pores and closed pores. After sintering, samples were densified range from 1100 to 1300 °C. The bulk density had been increased with increasing sintering temperatures. These curves indicated that densification increases of each grain boundary at 1100 °C to the maximum bulk densities at 1250 °C for 3 and 4 hours with samples Ca/P ratios of 1.65, 1.66, 1.67, 1.68 and 1.69. The densification curves of bulk density range from 1100 °C to 1200 °C observed that slight shrinkage of bodies and the phase formation of HA had a little changed. After sintering at 1250 °C and 1300 °C found that amount of HA phase increased because the heating rate of sintering increased while effect to β-TCP and CaO phase decreased. In addition, for 5 hours with samples Ca/P ratios of 1.67, 1.68 and 1.69 showed the maximum bulk densities was same. However, for samples sintered at 1300 °C with Ca/P ratios of 1.65, 1.66, 1.67, 1.68 and 1.69 for 2 hours indicated maximum bulk densities only and samples Ca/P ratios of 1.65 and 1.66 showed the maximum bulk densities for 5 hours was same. The maximum bulk densities of all condition when compared with the same temperature, its density indicated that a sintering at 1300 °C for 2 hours with samples Ca/P ratio of 1.69 was $2.38 \pm 0.03$ g/cm$^3$, which related with the apparent density due to highly porosity of sintered bodies.

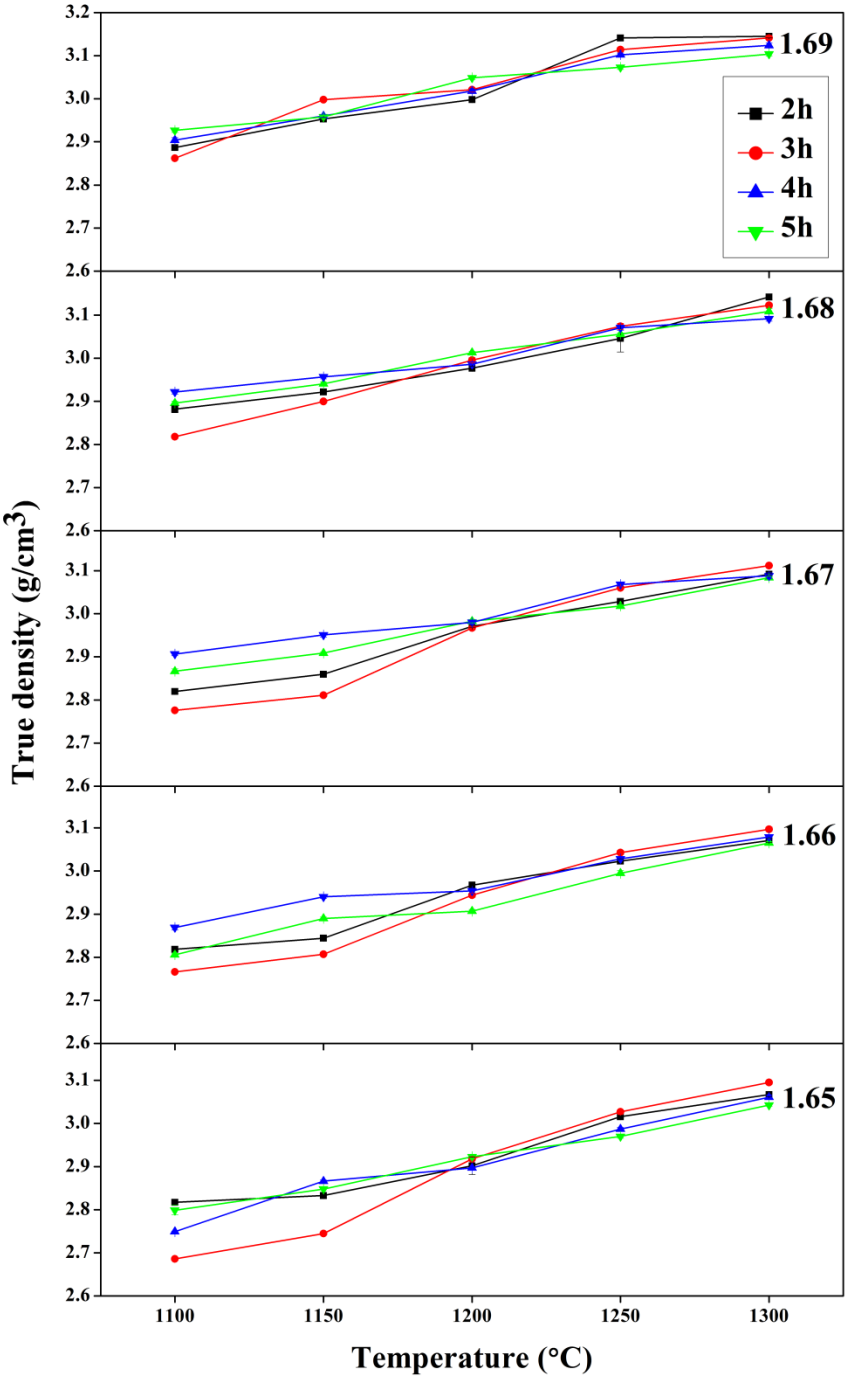


**Figure 17** True densities of Ca/P ratios 1.65, 1.66, 1.67, 1.68 and 1.69 at different temperatures and times.

**Figure 17** showed curves of the true density variation as a function of sintering temperatures. The true density included the solid component only. After sintering range from 1100 to 1300 °C, samples were densified and increased the density with increasing sintering temperatures. The maximum true densities at 1300 °C for 2, 3, 4 and 5 hours with samples Ca/P ratios of 1.65, 1.66, 1.67, 1.68 and 1.69 respectively. The maximum true densities of all condition when compared with the same sintering temperature indicated that a sintering at 1300 °C for 2 hours with samples Ca/P ratio of 1.69 was $3.145 \pm 0.002$ g/cm$^3$ which had value closest to the theoretical density.

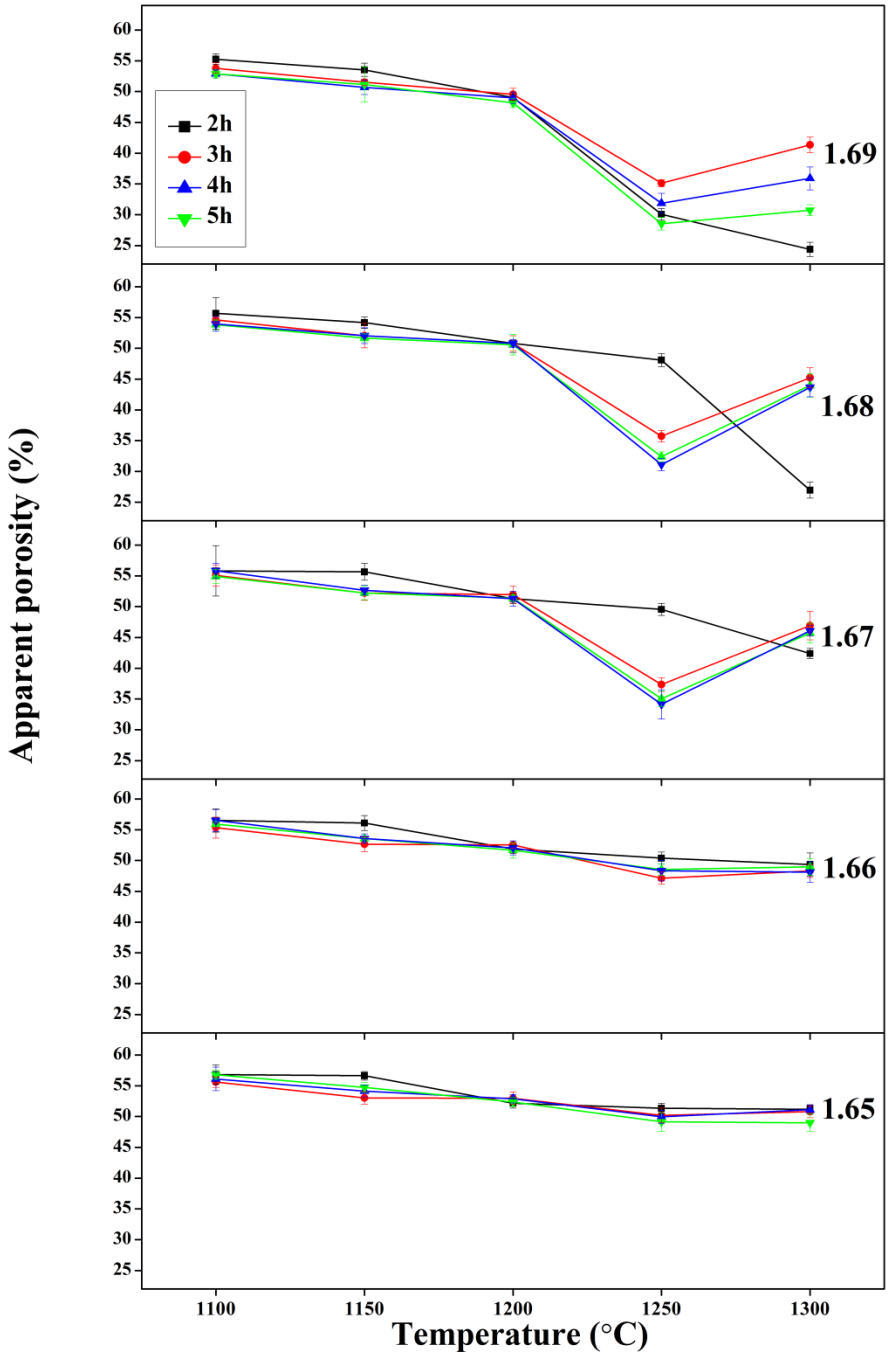


**Figure 18** Apparent porosities of Ca/P ratios 1.65, 1.66, 1.67, 1.68 and 1.69 at different temperatures and times.

**Figure 18** showed the relationship between sintering temperatures and apparent porosities. With increasing sintering temperature, both the bulk and apparent densities increases while the apparent porosity decrease as expected and the apparent porosity decreases with increasing the bulk and apparent density of which the maximum both densities had effect on the minimum apparent porosity. These curves indicated that shrinkage of samples increased due to the decrease of closed pores at 1100 °C was maximum porosity and became to the minimum porosity at 1250 °C for 3 and 4 hours with samples Ca/P ratios of 1.65, 1.66, 1.67, 1.68 and 1.69. In addition, for 5 hours with samples Ca/P ratios of 1.67, 1.68 and 1.69 showed the minimum porosity were same. In addition, for samples Ca/P ratios of 1.65 and 1.66 showed the minimum apparent porosity for 5 hours were same. However, for the samples sintered at 1300 °C with Ca/P ratios of 1.68 and 1.69 for 2 hours showed minimum apparent porosity when compared with other condition. The maximum bulk densities of all condition were affected on apparent porosity with the inversed curves of bulk density. From results, an apparent porosity with the same temperature indicated that sintering at 1300 °C for 2 hours with samples ratio of 1.69 had the minimum apparent porosity of $24.37 \pm 0.51$ % which related the maximum bulk density of samples.

### 3.4 Phase characterization of samples powder after sintered using XRD technique

Results of the XRD patterns of all sintered samples with various of Ca/P mole ratios, temperatures and times are shown in **Figure 19-23**.

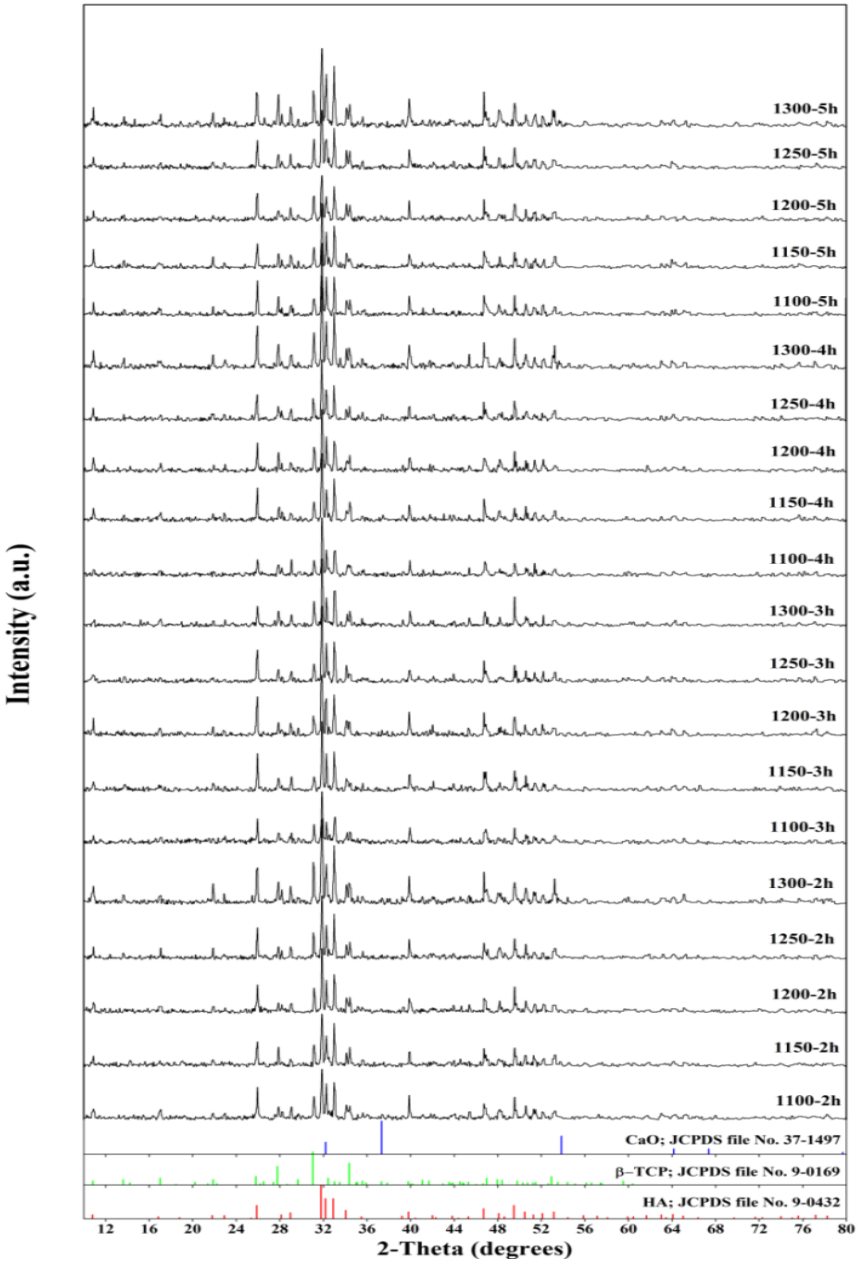


**Figure 19** XRD patterns of sample powders with Ca/P ratio 1.65 at different temperatures and times compared with standard JCPDS file of HA, β-TCP and CaO.

**Figure 19** showed the diffraction patterns of sintered samples with ratio of 1.65 at temperature range from 1100 to 1300 ˚C for 2 to 5 hours. The sintered samples were ceramics that consisted of mixtures of the HA, β-TCP and CaO phases. All sintered patterns were compared to the standard patterns JCPDS file no. 9-0432 of HA, JCPDS file no. 9-0169 of β-TCP and JCPDS file no. 37-1497 of CaO. The major peaks were HA phase and minor peaks were β-TCP and CaO for 2, 3, 4 and 5 hours. Peak of β-TCP was clearly seen from all diffraction patterns of samples powder while peak of CaO phase was difficult to seen. However, this phase could be observed the diffraction patterns of all samples. It seems that peaks intensities of HA increased with increasing of temperature which observed from increasing of intensity of HA peak. However, these results were not clear due to β-TCP peaks had trended increased when increased temperature were same with increased of HA peaks. For the influence of times on peak intensities were not clear because these peaks could not indicated trend of change peaks. These results had necessary to determined amount of phase content for identity of phase.

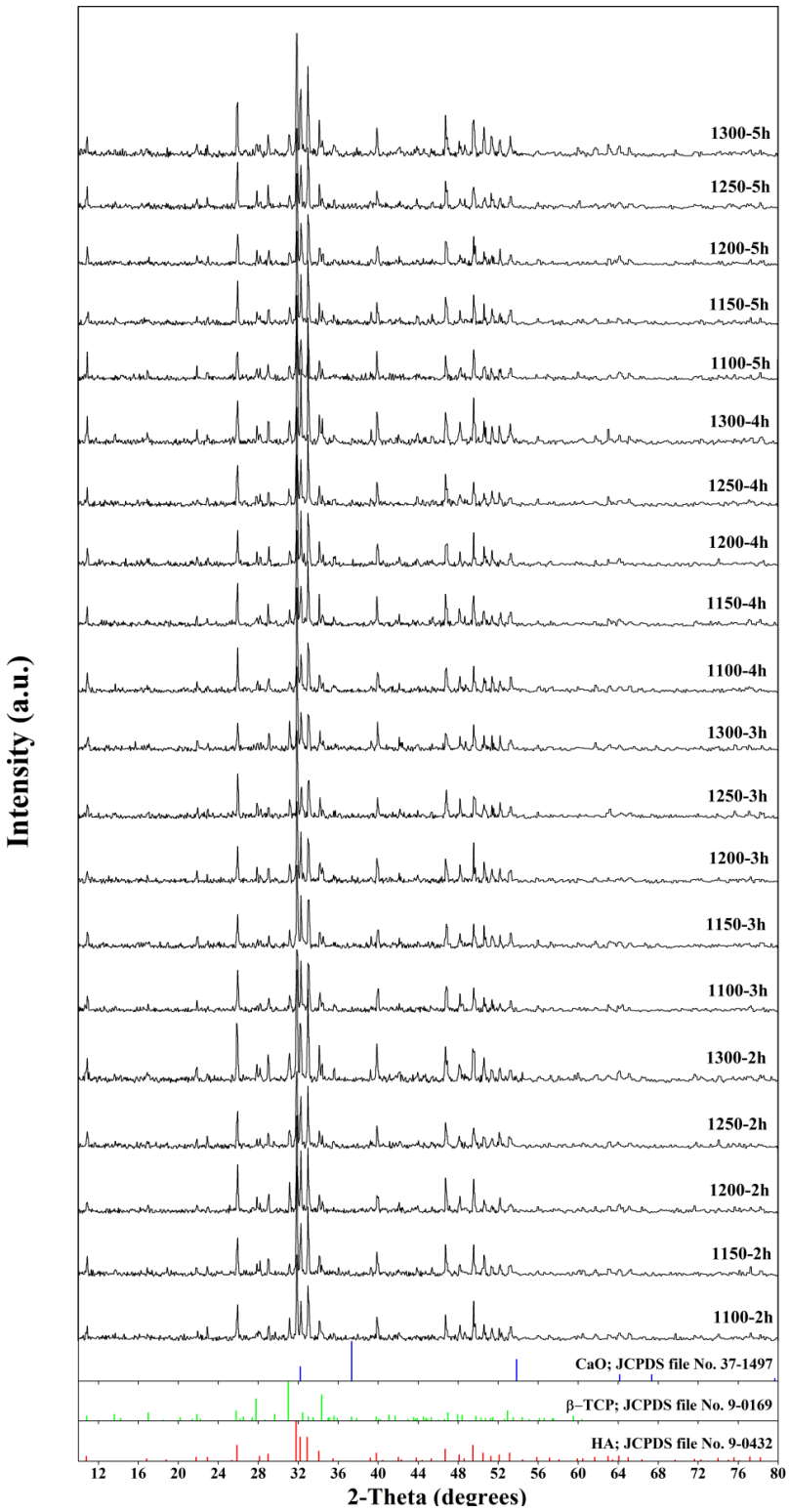


**Figure 20** XRD pattern of sample powders with Ca/P ratio 1.66 at different temperatures and times compared with standard JCPDS file of HA, β-TCP and CaO.

**Figure 20** showed the diffraction patterns of sintered samples with ratio of 1.66 at temperature range from 1100 ˚C to 1300 ˚C for 2 to 5 hours. The sintered samples were ceramics that contained of mixtures of the HA, β-TCP and CaO phases. The individual phase was compared to the standard patterns. The major peaks were HA phase and minor peaks were β-TCP and CaO for 2, 3, 4 and 5 hours. Peaks of β-TCP was still clearly seen from all diffraction patterns of samples powder and peaks of CaO phase was still difficult to see and remained appeared in the diffraction patterns of all samples. Moreover, the peak intensities of β-TCP with Ca/P ratio 1.66 had peak intensities of β-TCP lower than of sample with ratio of 1.65 at the same temperature and time. These results might cause from decreasing of phosphorus in composition and effect on decreasing of the peak intensities of β-TCP. Thus, the increased of Ca/P ratio had influence on increasing of HA phase at sintering temperature range from 1100 ˚C to 1300 ˚C because β-TCP peaks were decreased in all conditions. For the influence of times on peak intensities were not clear because influence of Ca/P ratio and temperature had more than the soaking time.

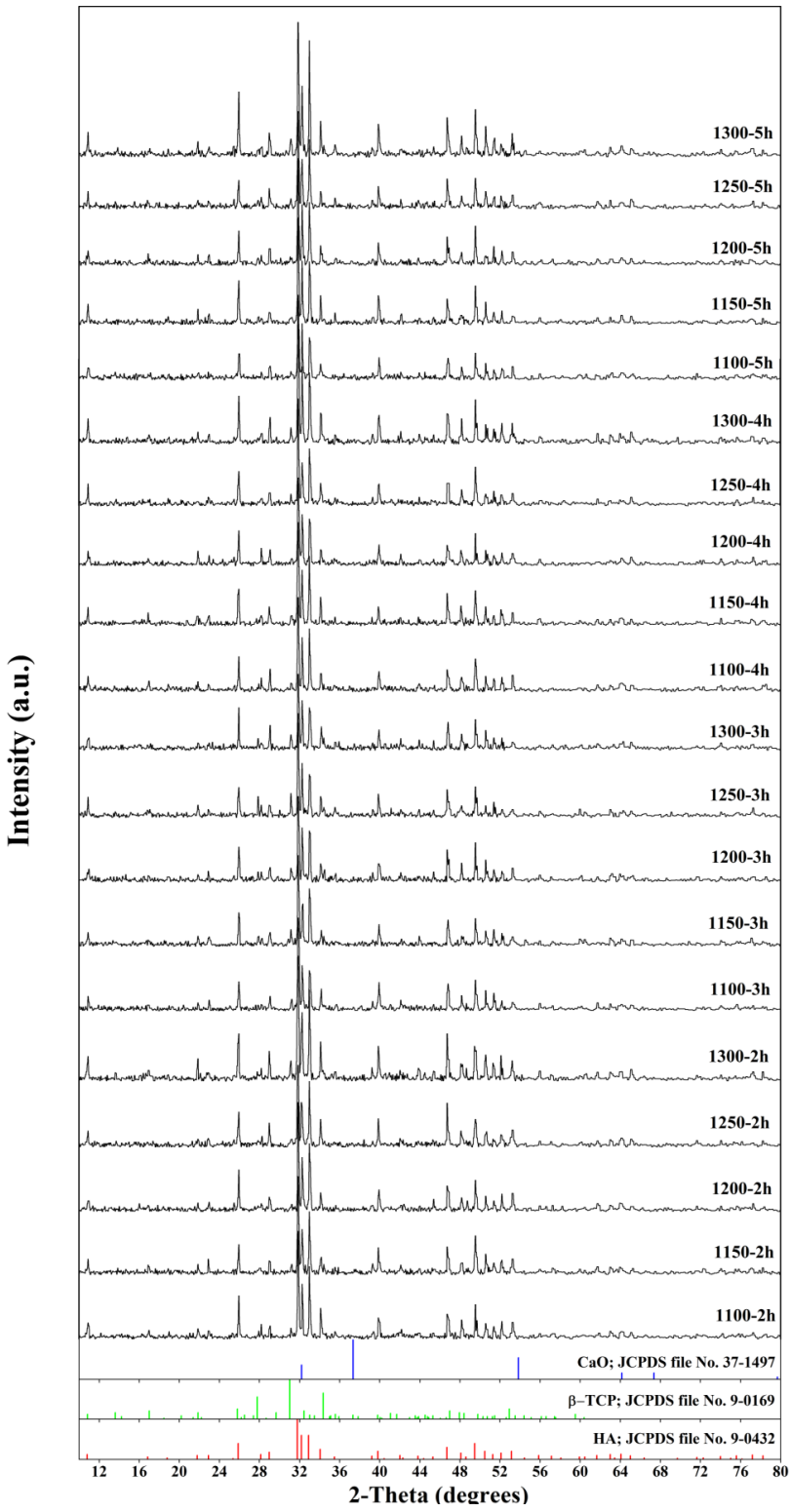


**Figure 21** XRD pattern of sample powders with Ca/P ratio 1.67 at different temperatures and times compared with standard JCPDS file of HA, β-TCP and CaO.

**Figure 21** showed the diffraction patterns of sintered samples with Ca/P ratio of 1.67 at temperature range from 1100 ˚C to 1300 ˚C for 2 to 5 hours. The sintered samples were ceramics that consisted of mixtures of the HA, β-TCP and CaO phases. All patterns were the same with Ca/P ratios of 1.65 and 1.66. The peak intensities of sample with ratio of 1.67 had peak intensities of β-TCP lower than of sample with ratios of 1.65 and 1.66 at the same temperature and time. At this ratio, it was found that peak intensities of β-TCP decreased with the increased of Ca/P ratio and temperature. Among the different of Ca/P ratios of 1.65, 1.66 and 1.67 at 1100 to 1300 for 2 to 5 hours, sample with ratio of 1.67 gave the maximum peak intensity of HA phase at the same temperature and time.

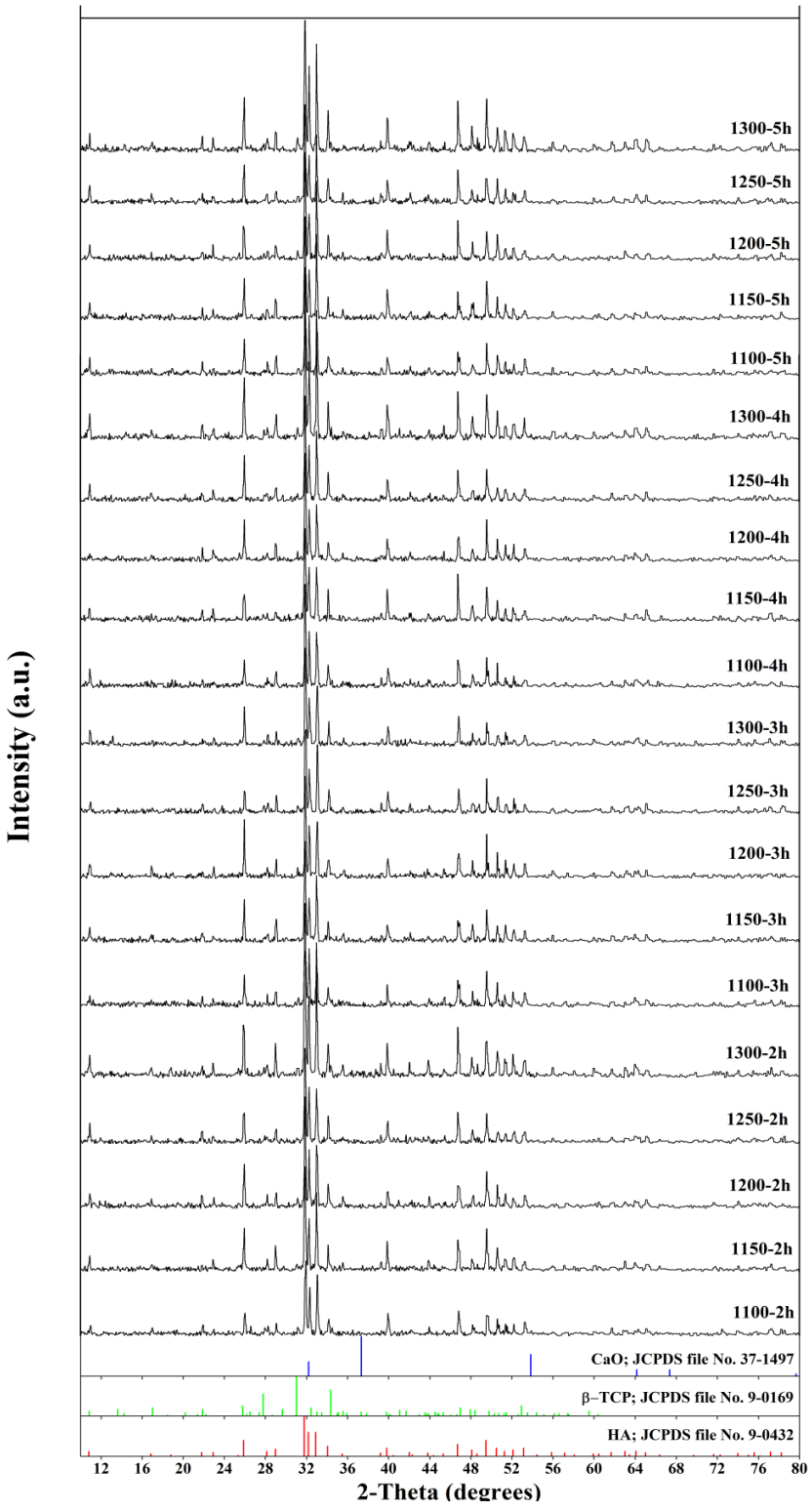


**Figure 22** XRD pattern of sample powders with Ca/P ratio 1.68 at different temperatures and times compared with standard JCPDS file of HA, β-TCP and CaO.

**Figure 22** showed the diffraction patterns of sintered samples with Ca/P ratio of 1.68 at temperature range from 1100 ˚C to 1300 ˚C for 2 to 5 hours. The sintered samples were ceramics that consisted of mixtures of the HA, β-TCP and CaO phases. These patterns were the same with Ca/P ratios of 1.65, 1.66 and 1.67. The peak intensities of sample with ratio of 1.68 had peak intensities of β-TCP lower than of sample with ratios of 1.65, 1.66 and 1.67 at the same temperature and time. At this ratio, it was found that peak intensities of β-TCP decreased with the increased of Ca/P ratio and temperature. Among the different of Ca/P ratios of 1.65, 1.66, 1.67 and 1.68 at 1100 to 1300 for 2 to 5 hours, sample with ratio of 1.68 gave the maximum peak intensity of HA phase at the same temperature and time.

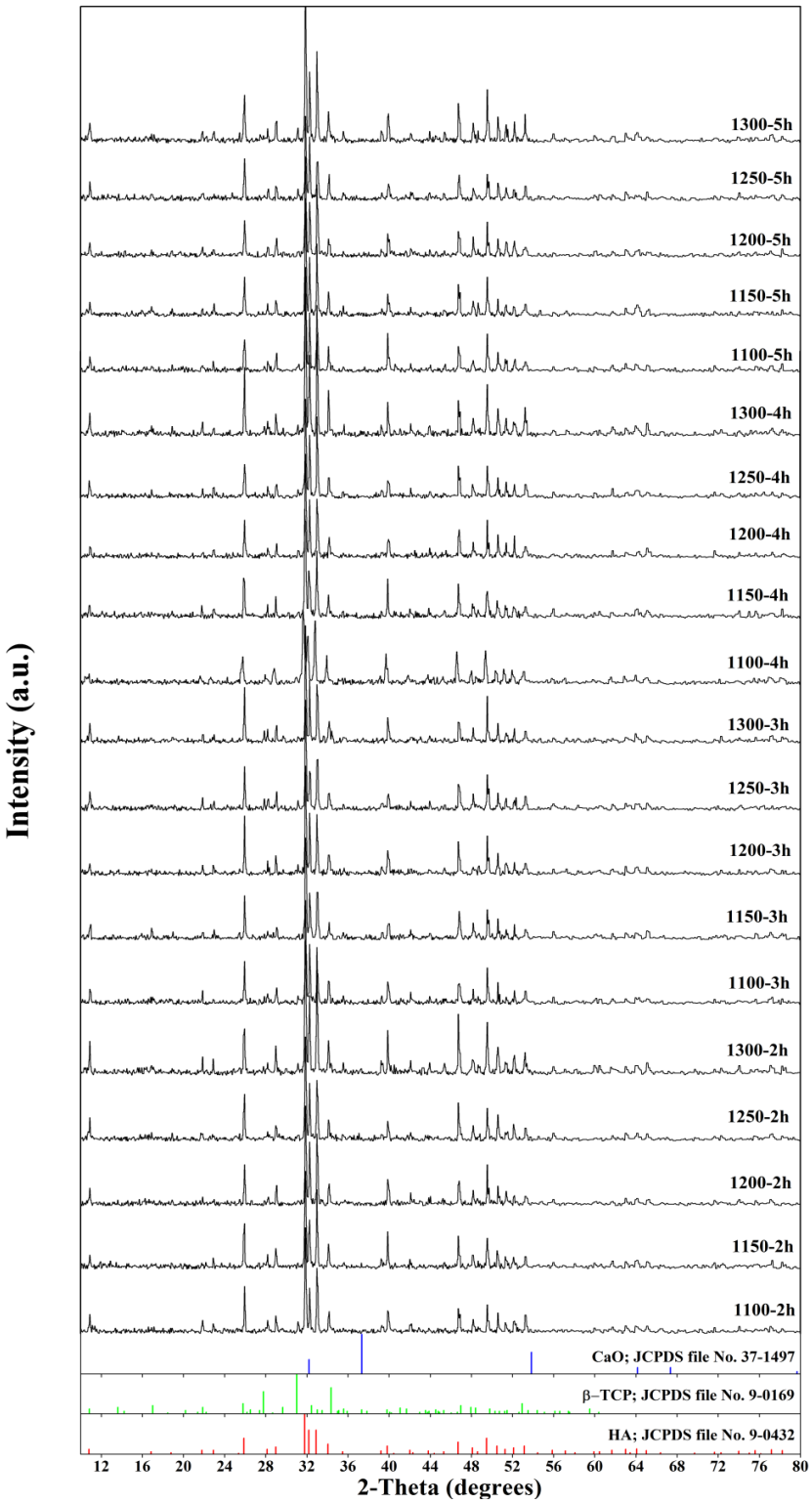


**Figure 23** XRD pattern of sample powders with Ca/P ratio 1.69 at different temperatures and times compared with standard JCPDS file of HA, β-TCP and CaO.

**Figure 23** showed the diffraction patterns of sintered samples with Ca/P ratio of 1.69 at temperature range from 1100 ˚C to 1300 ˚C for 2 to 5 hours. The sintered samples were ceramics that consisted of mixtures of the HA, β-TCP and CaO phases. These patterns were the same with Ca/P ratios of 1.65, 1.66, 1.67 and 1.68. The peak intensities of sample with ratio of 1.69 had intensities of β-TCP lower than of sample with ratios of 1.65, 1.66, 1.67 and 1.68 at the same temperature and time. At this ratio, it was found that peak intensities of β-TCP decreased with the increased of Ca/P ratio and temperature. Among the different of Ca/P ratios of 1.65, 1.66, 1.67, 1.68 and 1.69 at 1100 to 1300 °C for 2 to 5 hours, sample with ratio of 1.69 gave the maximum peak intensity of HA phase when compared with other condition. For the influence of various times on intensities were not clear due to have not seen change.

The percentages of volume fraction of HA, TCP and CaO presented in **Table 6**. These amounts were calculated using the relative intensity ratio (RIR) of the main diffraction peaks of HA (**equation 16**). The peaks were indexed according to the standard patterns JCPDS file. These patterns fits the relative intensities of the five dominant HA peaks found at 2θ = 25.88°, 31.78°, 32.18°, 32.90° and 49.472°. For the five dominant β-TCP peaks found at 2θ = 27.77°, 31.02°, 34.37°, 46.97° and 52.94°. For the five dominant CaO peaks found at 2θ = 37.36°, 53.85°, 64.16°, 67.36° and 79.66°.

$$\% \text{ phase content} = \left(\frac{I_{\beta-TCP}}{I_{\beta-TCP}+I_{HA}+I_{CaO}}\right) \times 100 \qquad (16)$$

where, $I_{\beta\text{-TCP}}$ = Sum of first 5 highest intensity in β-TCP phase

$I_{HA}$ = Sum of first 5 highest intensity in HA phase

$I_{CaO}$ = Sum of first 5 highest intensity in CaO phase

Results of phase contents of sintered sample with various of Ca/P mole ratios, temperatures and soaking times are shown in **Table 6**.

**Table 6** Phase composition of all sintered samples

| Sample | Percentage of HA, β-TCP and CaO phases in sintered samples | | |
|---|---|---|---|
| | HA | TCP | CaO |
| 1A-2 | 67.44 | 25.91 | 6.64 |
| 1B-2 | 67.75 | 24.94 | 7.31 |
| 1C-2 | 67.85 | 27.47 | 5.14 |
| 1D-2 | 68.83 | 23.41 | 7.76 |
| 1E-2 | 69.13 | 25.10 | 5.76 |
| 1A-3 | 64.29 | 27.62 | 8.08 |
| 1B-3 | 66.56 | 25.55 | 7.89 |
| 1C-3 | 72.07 | 21.56 | 6.37 |
| 1D-3 | 72.66 | 21.60 | 5.74 |
| 1E-3 | 78.77 | 13.04 | 5.99 |
| 1A-4 | 70.53 | 25.86 | 3.62 |
| 1B-4 | 70.64 | 23.96 | 5.40 |
| 1C-4 | 70.81 | 21.16 | 8.04 |
| 1D-4 | 71.07 | 22.95 | 5.99 |
| 1E-4 | 73.33 | 18.22 | 8.45 |
| 1A-5 | 63.59 | 30.53 | 5.88 |
| 1B-5 | 64.28 | 26.49 | 9.22 |
| 1C-5 | 66.25 | 30.05 | 3.69 |
| 1D-5 | 69.76 | 24.07 | 6.17 |
| 1E-5 | 70.54 | 23.00 | 6.46 |

**Table 6** (Cont'd)

| Sample | Percentage of HA, β-TCP and CaO phases in sintered samples | | |
|---|---|---|---|
| | HA | TCP | CaO |
| 2A-2 | 76.67 | 16.60 | 6.73 |
| 2B-2 | 79.13 | 14.98 | 5.89 |
| 2C-2 | 79.62 | 15.59 | 4.80 |
| 2D-2 | 81.28 | 15.37 | 3.36 |
| 2E-2 | 87.67 | 7.43 | 4.90 |
| 2A-3 | 73.15 | 18.08 | 8.77 |
| 2B-3 | 74.09 | 19.30 | 6.61 |
| 2C-3 | 76.57 | 18.44 | 4.99 |
| 2D-3 | 81.89 | 12.64 | 5.47 |
| 2E-3 | 84.73 | 8.97 | 6.30 |
| 2A-4 | 77.08 | 19.21 | 3.70 |
| 2B-4 | 78.56 | 14.58 | 6.86 |
| 2C-4 | 79.87 | 14.33 | 5.80 |
| 2D-4 | 82.24 | 12.73 | 5.03 |
| 2E-4 | 84.82 | 8.82 | 6.36 |
| 2A-5 | 75.26 | 18.19 | 6.54 |
| 2B-5 | 78.18 | 15.52 | 6.29 |
| 2C-5 | 79.10 | 14.49 | 6.41 |
| 2D-5 | 80.24 | 13.33 | 6.43 |
| 2E-5 | 87.20 | 8.70 | 4.10 |
| 3A-2 | 82.32 | 12.76 | 4.92 |
| 3B-2 | 84.64 | 9.08 | 6.28 |
| 3C-2 | 85.64 | 8.78 | 5.57 |
| 3D-2 | 86.45 | 9.71 | 3.84 |
| 3E-2 | 88.78 | 7.50 | 3.73 |

**Table 6** (Cont'd)

| Sample | Percentage of HA, β-TCP and CaO phases in sintered samples | | |
|---|---|---|---|
| | HA | TCP | CaO |
| 3A-3 | 74.82 | 18.36 | 6.83 |
| 3B-3 | 78.77 | 14.74 | 6.49 |
| 3C-3 | 79.84 | 13.56 | 6.60 |
| 3D-3 | 84.33 | 9.67 | 5.99 |
| 3E-3 | 86.97 | 7.97 | 5.06 |
| 3A-4 | 80.02 | 10.38 | 9.60 |
| 3B-4 | 83.27 | 10.61 | 6.12 |
| 3C-4 | 84.91 | 9.30 | 5.79 |
| 3D-4 | 86.80 | 9.56 | 3.64 |
| 3E-4 | 88.73 | 6.59 | 4.68 |
| 3A-5 | 82.26 | 10.15 | 7.59 |
| 3B-5 | 83.94 | 10.36 | 5.70 |
| 3C-5 | 84.88 | 9.87 | 5.26 |
| 3D-5 | 85.93 | 7.91 | 6.16 |
| 3E-5 | 88.23 | 6.44 | 5.33 |
| 4A-2 | 83.40 | 10.63 | 5.97 |
| 4B-2 | 84.65 | 9.04 | 6.31 |
| 4C-2 | 85.88 | 8.10 | 6.02 |
| 4D-2 | 89.61 | 5.97 | 4.42 |
| 4E-2 | 91.06 | 6.24 | 2.70 |
| 4A-3 | 85.03 | 7.76 | 7.21 |
| 4B-3 | 86.01 | 7.83 | 6.15 |
| 4C-3 | 86.16 | 7.55 | 6.29 |
| 4D-3 | 86.39 | 9.65 | 3.96 |
| 4E-3 | 90.57 | 5.47 | 3.97 |

**Table 6** (Cont'd)

| Sample | Percentage of HA, β-TCP and CaO phases in sintered samples | | |
|---|---|---|---|
| | HA | TCP | CaO |
| 4A-4 | 83.65 | 8.87 | 7.49 |
| 4B-4 | 86.07 | 8.08 | 5.85 |
| 4C-4 | 86.32 | 7.04 | 6.64 |
| 4D-4 | 88.31 | 7.51 | 4.18 |
| 4E-4 | 89.84 | 4.23 | 5.93 |
| 4A-5 | 83.79 | 8.71 | 7.50 |
| 4B-5 | 84.22 | 9.84 | 5.94 |
| 4C-5 | 85.27 | 10.19 | 4.54 |
| 4D-5 | 87.06 | 8.24 | 4.69 |
| 4E-5 | 89.24 | 7.42 | 3.34 |
| 5A-2 | 85.91 | 8.50 | 5.59 |
| 5B-2 | 89.10 | 5.49 | 5.40 |
| 5C-2 | 89.86 | 4.24 | 5.90 |
| 5D-2 | 91.23 | 5.27 | 3.51 |
| 5E-2 | 91.44 | 5.18 | 3.38 |
| 5A-3 | 85.66 | 6.19 | 8.15 |
| 5B-3 | 87.26 | 7.67 | 5.07 |
| 5C-3 | 89.67 | 7.11 | 3.22 |
| 5D-3 | 90.27 | 5.67 | 4.06 |
| 5E-3 | 91.02 | 4.51 | 4.47 |
| 5A-4 | 84.83 | 9.79 | 5.38 |
| 5B-4 | 86.98 | 7.84 | 5.18 |
| 5C-4 | 88.15 | 5.08 | 6.77 |
| 5D-4 | 89.92 | 4.97 | 5.11 |
| 5E-4 | 90.54 | 4.70 | 4.75 |

**Table 6** (Cont'd)

| Sample | Percentage of HA, β-TCP and CaO phases in sintered samples | | |
|---|---|---|---|
| | HA | TCP | CaO |
| 5A-5 | 85.73 | 9.39 | 4.87 |
| 5B-5 | 87.20 | 8.62 | 4.18 |
| 5C-5 | 88.61 | 7.14 | 4.25 |
| 5D-5 | 89.02 | 6.61 | 4.37 |
| 5E-5 | 89.98 | 4.01 | 6.00 |

**Figure 24** showed sintered sample with ratio of 1.65 to 1.69 at temperatures 1100 °C to 1300 °C for 2 to 5 hours of which evaluated from **Table 6**. These results found that when sintered at these temperatures had effect on the formation of HA and increasing of this phases correspond to increasing of isothermal temperature. For the sample with ratio 1.65 was found that the increasing of HA phase at temperatures range 1100 °C to 1200 °C for 2 and 4 hours had a very little changed to HA due to observed from the slope of curves which had a small slope and after sintering up to 1250 °C and 1300 °C occurred that HA phase increased but not much. For 3 and 5 hours was found that the formation of HA phase had more when compared with 2 and 4 hours at temperatures range 1100 °C to 1200 °C of which observed from slope of curves was higher and after sintered up to 1300 °C. This temperature for 3 hours had been the formation of maximum HA as 78.77 % and influence of times on phase formation could not be indicated due to constant of curves.

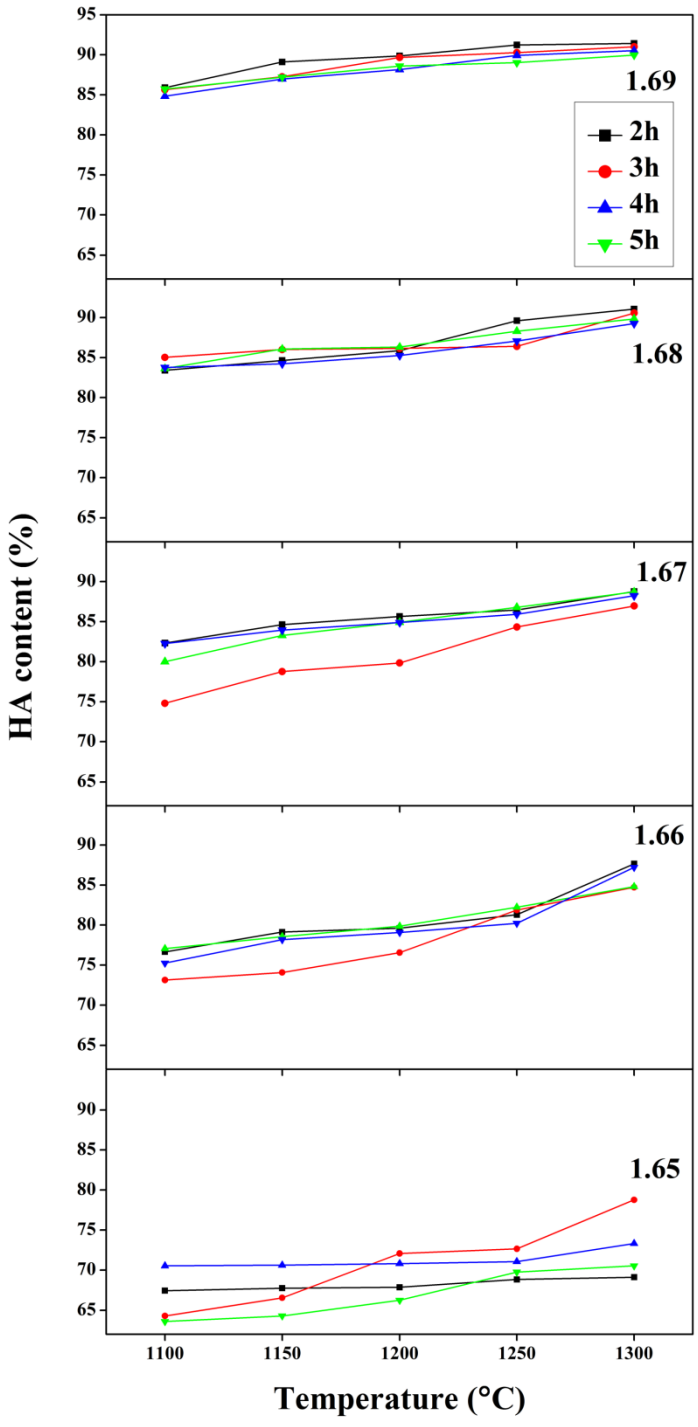


**Figure 24** HA contents of Ca/P ratios 1.65, 1.66, 1.67, 1.68 and 1.69 at different temperatures and times.

For the sample with ratio of 1.66 was found that the increasing of HA phase at temperature range from 1100 °C to 1200 °C for 2, 3, 4 and 5 hours. This ratio had been the formation of HA phase not much when sintered up to 1250 °C. At 1300 °C, it was found that amounts of HA phase increased with the increase of density and shrinkage of samples. This phase was 87.67 % at 1300 °C for 2 hours and observed that at temperature range from 1100 °C to 1200 °C for 3 hours had amounts of HA phase was minimum and outside of group.

For the sample with ratio of 1.67 was found that temperature had effect on phase formation of HA. This ratio was the same with ratio of 1.65 and 1.66. At temperatures range from 1100 °C to 1200 °C was found that the formation of HA phase not much until to 1250 °C and 1300 °C for 2, 4 and 5 hours. This phase had been change little when observed slope of curves except for 3 hours which clearly change phase. This composition had been the maximum phase of HA as 88.78 % at 1300 °C for 2 hours.

For the sample with ratio of 1.68 was found that temperature had effect on phase formation of HA. This ratio was the same with ratio of 1.65, 1.66 and 1.67. At temperatures range 1100 °C to 1200 °C was found that the formation of HA phase not much until to 1250 °C and 1300 °C, which observed HA phase of maximum as 91.06 % at 1300 °C for 2 hours and influence of times was not much effect on the phase HA due to not different of curves.

For the sample with ratio of 1.69 was found that temperature had effect on phase formation of HA. This ratio was the same with ratio of 1.65, 1.66, 1.67 and 1.68. At temperatures range 1100 °C to 1200 °C was found that the formation of HA phase not much until to 1250 °C and 1300 °C, which observed that HA phase of maximum was 91.44 % at 1300 °C for 2 hours and influence of soaking times was not much effected on the phase formation due to not different of curves. This value was the maximum percentage of HA phase which compared with theory of single phase HA 95 % and the composition of Ca/P ratio was important parameter for HA synthesized.

### 3.5 Chemical properties of sintered samples.

3.5.1 Chemical analysis (XRF) of sintered samples with various of Ca/P mole ratios, temperatures and times showed in **Table 7**

**Table 7** The Ca/P mole ratios and total elements of all sintered samples

| Sample | Content (% w/w) | | | | | Ca/P |
|---|---|---|---|---|---|---|
| | Ca | P | Si | Sr | Na | (Mole ratio) |
| 1A-2 | 66.39 | 32.51 | 0.77 | 0.33 | < 0.01 | 1.579 |
| 1B-2 | 66.35 | 32.55 | 0.77 | 0.33 | < 0.01 | 1.576 |
| 1C-2 | 66.60 | 32.30 | 0.73 | 0.36 | < 0.01 | 1.594 |
| 1D-2 | 66.34 | 32.56 | 0.75 | 0.36 | < 0.01 | 1.575 |
| 1E-2 | 66.51 | 32.42 | 0.74 | 0.33 | < 0.01 | 1.586 |
| 1A-3 | 66.19 | 32.67 | 0.83 | 0.32 | < 0.01 | 1.566 |
| 1B-3 | 66.26 | 32.60 | 0.83 | 0.31 | < 0.01 | 1.571 |
| 1C-3 | 66.47 | 32.37 | 0.79 | 0.38 | < 0.01 | 1.588 |
| 1D-3 | 66.57 | 32.33 | 0.76 | 0.34 | < 0.01 | 1.592 |
| 1E-3 | 66.28 | 32.69 | 0.71 | 0.31 | < 0.01 | 1.567 |
| 1A-4 | 66.69 | 32.24 | 0.73 | 0.34 | < 0.01 | 1.599 |
| 1B-4 | 66.57 | 32.36 | 0.73 | 0.33 | < 0.01 | 1.590 |
| 1C-4 | 66.36 | 32.52 | 0.75 | 0.37 | < 0.01 | 1.577 |
| 1D-4 | 66.51 | 32.38 | 0.78 | 0.33 | < 0.01 | 1.588 |
| 1E-4 | 66.43 | 32.52 | 0.74 | 0.31 | < 0.01 | 1.579 |
| 1A-5 | 66.27 | 32.50 | 0.87 | 0.35 | < 0.01 | 1.576 |
| 1B-5 | 66.06 | 32.73 | 0.86 | 0.35 | < 0.01 | 1.561 |
| 1C-5 | 66.53 | 32.32 | 0.77 | 0.37 | < 0.01 | 1.591 |
| 1D-5 | 66.44 | 32.41 | 0.78 | 0.37 | < 0.01 | 1.585 |
| 1E-5 | 66.49 | 32.44 | 0.73 | 0.34 | < 0.01 | 1.585 |

**Table 7** (Cont'd)

| Sample | Content (%w/w) | | | | | Ca/P |
|---|---|---|---|---|---|---|
| | Ca | P | Si | Sr | Na | (Mole ratio) |
| 2A-2 | 66.61 | 32.32 | 0.73 | 0.34 | < 0.01 | 1.593 |
| 2B-2 | 66.74 | 32.22 | 0.73 | 0.31 | < 0.01 | 1.602 |
| 2C-2 | 66.81 | 32.12 | 0.75 | 0.32 | < 0.01 | 1.608 |
| 2D-2 | 66.94 | 31.99 | 0.74 | 0.33 | < 0.01 | 1.618 |
| 2E-2 | 66.86 | 31.90 | 0.89 | 0.35 | < 0.01 | 1.620 |
| 2A-3 | 66.39 | 32.54 | 0.74 | 0.33 | < 0.01 | 1.577 |
| 2B-3 | 66.55 | 32.36 | 0.73 | 0.35 | < 0.01 | 1.590 |
| 2C-3 | 66.74 | 32.21 | 0.73 | 0.32 | < 0.01 | 1.602 |
| 2D-3 | 66.79 | 32.11 | 0.76 | 0.34 | < 0.01 | 1.608 |
| 2E-3 | 66.72 | 32.06 | 0.88 | 0.33 | < 0.01 | 1.609 |
| 2A-4 | 66.81 | 32.10 | 0.75 | 0.35 | < 0.01 | 1.609 |
| 2B-4 | 66.64 | 32.28 | 0.74 | 0.34 | < 0.01 | 1.596 |
| 2C-4 | 66.75 | 32.19 | 0.74 | 0.33 | < 0.01 | 1.603 |
| 2D-4 | 66.85 | 32.08 | 0.75 | 0.32 | < 0.01 | 1.611 |
| 2E-4 | 66.83 | 32.12 | 0.73 | 0.31 | < 0.01 | 1.608 |
| 2A-5 | 66.60 | 32.34 | 0.72 | 0.33 | < 0.01 | 1.592 |
| 2B-5 | 66.68 | 32.26 | 0.73 | 0.33 | < 0.01 | 1.598 |
| 2C-5 | 66.67 | 32.24 | 0.74 | 0.35 | < 0.01 | 1.599 |
| 2D-5 | 66.71 | 32.22 | 0.73 | 0.34 | < 0.01 | 1.601 |
| 2E-5 | 67.03 | 31.92 | 0.73 | 0.32 | < 0.01 | 1.624 |

**Table 7** (Cont'd)

| Sample | Content (%w/w) | | | | | Ca/P |
|---|---|---|---|---|---|---|
| | Ca | P | Si | Sr | Na | (Mole ratio) |
| 3A-2 | 66.77 | 32.03 | 0.74 | 0.46 | < 0.01 | 1.612 |
| 3B-2 | 66.73 | 32.07 | 0.73 | 0.47 | < 0.01 | 1.609 |
| 3C-2 | 66.83 | 32.02 | 0.82 | 0.34 | < 0.01 | 1.614 |
| 3D-2 | 66.99 | 31.89 | 0.78 | 0.34 | < 0.01 | 1.624 |
| 3E-2 | 67.08 | 31.85 | 0.73 | 0.34 | < 0.01 | 1.628 |
| 3A-3 | 66.49 | 32.33 | 0.72 | 0.46 | < 0.01 | 1.590 |
| 3B-3 | 66.61 | 32.23 | 0.71 | 0.46 | < 0.01 | 1.598 |
| 3C-3 | 66.62 | 32.21 | 0.73 | 0.44 | < 0.01 | 1.599 |
| 3D-3 | 66.81 | 32.09 | 0.76 | 0.33 | < 0.01 | 1.609 |
| 3E-3 | 66.92 | 31.96 | 0.75 | 0.37 | < 0.01 | 1.618 |
| 3A-4 | 66.39 | 32.39 | 0.73 | 0.48 | < 0.01 | 1.584 |
| 3B-4 | 66.73 | 32.10 | 0.72 | 0.44 | < 0.01 | 1.607 |
| 3C-4 | 66.77 | 32.03 | 0.75 | 0.45 | < 0.01 | 1.611 |
| 3D-4 | 67.00 | 31.87 | 0.78 | 0.35 | < 0.01 | 1.625 |
| 3E-4 | 66.97 | 31.89 | 0.80 | 0.33 | < 0.01 | 1.623 |
| 3A-5 | 66.68 | 32.26 | 0.68 | 0.38 | < 0.01 | 1.598 |
| 3B-5 | 66.77 | 32.06 | 0.72 | 0.46 | < 0.01 | 1.610 |
| 3C-5 | 66.85 | 32.02 | 0.73 | 0.41 | < 0.01 | 1.614 |
| 3D-5 | 66.83 | 32.07 | 0.78 | 0.32 | < 0.01 | 1.611 |
| 3E-5 | 66.87 | 31.93 | 0.88 | 0.33 | < 0.01 | 1.619 |

**Table 7** (Cont'd)

| Sample | Content (%w/w) | | | | | Ca/P |
|---|---|---|---|---|---|---|
| | Ca | P | Si | Sr | Na | (Mole ratio) |
| 4A-2 | 66.80 | 32.12 | 0.69 | 0.39 | < 0.01 | 1.608 |
| 4B-2 | 66.82 | 32.11 | 0.70 | 0.38 | < 0.01 | 1.608 |
| 4C-2 | 66.78 | 32.03 | 0.76 | 0.43 | < 0.01 | 1.612 |
| 4D-2 | 67.00 | 31.85 | 0.82 | 0.33 | < 0.01 | 1.626 |
| 4E-2 | 67.08 | 31.68 | 0.85 | 0.39 | < 0.01 | 1.637 |
| 4A-3 | 66.81 | 32.19 | 0.60 | 0.41 | < 0.01 | 1.605 |
| 4B-3 | 66.88 | 32.09 | 0.69 | 0.33 | < 0.01 | 1.611 |
| 4C-3 | 66.78 | 32.05 | 0.83 | 0.35 | < 0.01 | 1.611 |
| 4D-3 | 66.91 | 31.87 | 0.85 | 0.38 | < 0.01 | 1.623 |
| 4E-3 | 67.09 | 31.82 | 0.76 | 0.33 | < 0.01 | 1.630 |
| 4A-4 | 66.72 | 32.22 | 0.65 | 0.41 | < 0.01 | 1.601 |
| 4B-4 | 66.89 | 32.06 | 0.69 | 0.37 | < 0.01 | 1.613 |
| 4C-4 | 66.78 | 32.07 | 0.83 | 0.32 | < 0.01 | 1.610 |
| 4D-4 | 66.95 | 31.85 | 0.84 | 0.36 | < 0.01 | 1.625 |
| 4E-4 | 66.85 | 31.92 | 0.88 | 0.36 | < 0.01 | 1.619 |
| 4A-5 | 66.64 | 32.18 | 0.73 | 0.46 | < 0.01 | 1.601 |
| 4B-5 | 66.84 | 32.10 | 0.67 | 0.38 | < 0.01 | 1.610 |
| 4C-5 | 66.90 | 31.96 | 0.82 | 0.33 | < 0.01 | 1.618 |
| 4D-5 | 66.87 | 31.90 | 0.85 | 0.38 | < 0.01 | 1.620 |
| 4E-5 | 67.07 | 31.80 | 0.82 | 0.32 | < 0.01 | 1.631 |

**Table 7** (Cont'd)

| Sample | Content (%w/w) | | | | | Ca/P |
|---|---|---|---|---|---|---|
| | Ca | P | Si | Sr | Na | (Mole ratio) |
| 5A-2 | 66.94 | 32.06 | 0.58 | 0.41 | < 0.01 | 1.614 |
| 5B-2 | 67.02 | 31.98 | 0.59 | 0.41 | < 0.01 | 1.620 |
| 5C-2 | 67.04 | 32.01 | 0.63 | 0.32 | < 0.01 | 1.619 |
| 5D-2 | 67.24 | 31.82 | 0.63 | 0.31 | < 0.01 | 1.633 |
| 5E-2 | 67.13 | 31.76 | 0.77 | 0.34 | < 0.01 | 1.634 |
| 5A-3 | 66.74 | 32.23 | 0.68 | 0.36 | < 0.01 | 1.601 |
| 5B-3 | 67.00 | 31.99 | 0.60 | 0.41 | < 0.01 | 1.619 |
| 5C-3 | 67.22 | 31.84 | 0.63 | 0.30 | < 0.01 | 1.632 |
| 5D-3 | 67.17 | 31.88 | 0.63 | 0.32 | < 0.01 | 1.629 |
| 5E-3 | 67.03 | 31.83 | 0.81 | 0.33 | < 0.01 | 1.628 |
| 5A-4 | 66.92 | 32.07 | 0.60 | 0.41 | < 0.01 | 1.613 |
| 5B-4 | 66.97 | 32.00 | 0.60 | 0.43 | < 0.01 | 1.618 |
| 5C-4 | 66.94 | 32.10 | 0.65 | 0.31 | < 0.01 | 1.612 |
| 5D-4 | 67.07 | 31.95 | 0.64 | 0.35 | < 0.01 | 1.623 |
| 5E-4 | 67.03 | 31.88 | 0.78 | 0.31 | < 0.01 | 1.626 |
| 5A-5 | 66.97 | 32.01 | 0.60 | 0.42 | < 0.01 | 1.617 |
| 5B-5 | 67.08 | 31.95 | 0.55 | 0.41 | < 0.01 | 1.623 |
| 5C-5 | 67.11 | 31.92 | 0.63 | 0.33 | < 0.01 | 1.625 |
| 5D-5 | 67.14 | 31.94 | 0.61 | 0.31 | < 0.01 | 1.625 |
| 5E-5 | 66.93 | 31.97 | 0.77 | 0.34 | < 0.01 | 1.619 |

The elements were detected by XRF in **Table 7**. The Ca/P mole ratios showed in this table also confirmed the accuracy of the results obtained during this study from the semi quantitative technique of determining the phase composition of the alls samples through the comparison of the XRD peak intensities of the final phases. The XRF results revealed that Ca/P mole ratios of these samples lower than the theoretical value of 1.67. All samples were contained the main element of calcium and phosphorus. Minor elements were silicon and strontium. A trace element of sodium was found. The chemical formula corresponds to the after mentioned chemical analysis with considering the charge compensation of the deficient calcium by substituting $PO_4^{3-}$ with $CO_3^{2-}$ and creating a vacancy on $OH^-$ site which showed as followed $Ca_{10-x}V(PO_4)_{6-x}(CO_3)_x(OH)_{2-2x}O_xV_x$; the apatite network with the space group $P6_3/m$ can accepted different substitutions of their compositions producing substitutional impurities atoms and vacancies (V) if the ions replacing $Ca^{2+}$, $PO_4^{3-}$ and $OH^-$.

3.5.2 The IR spectra of sintered samples at different temperatures and soaking times in **Figure 25**

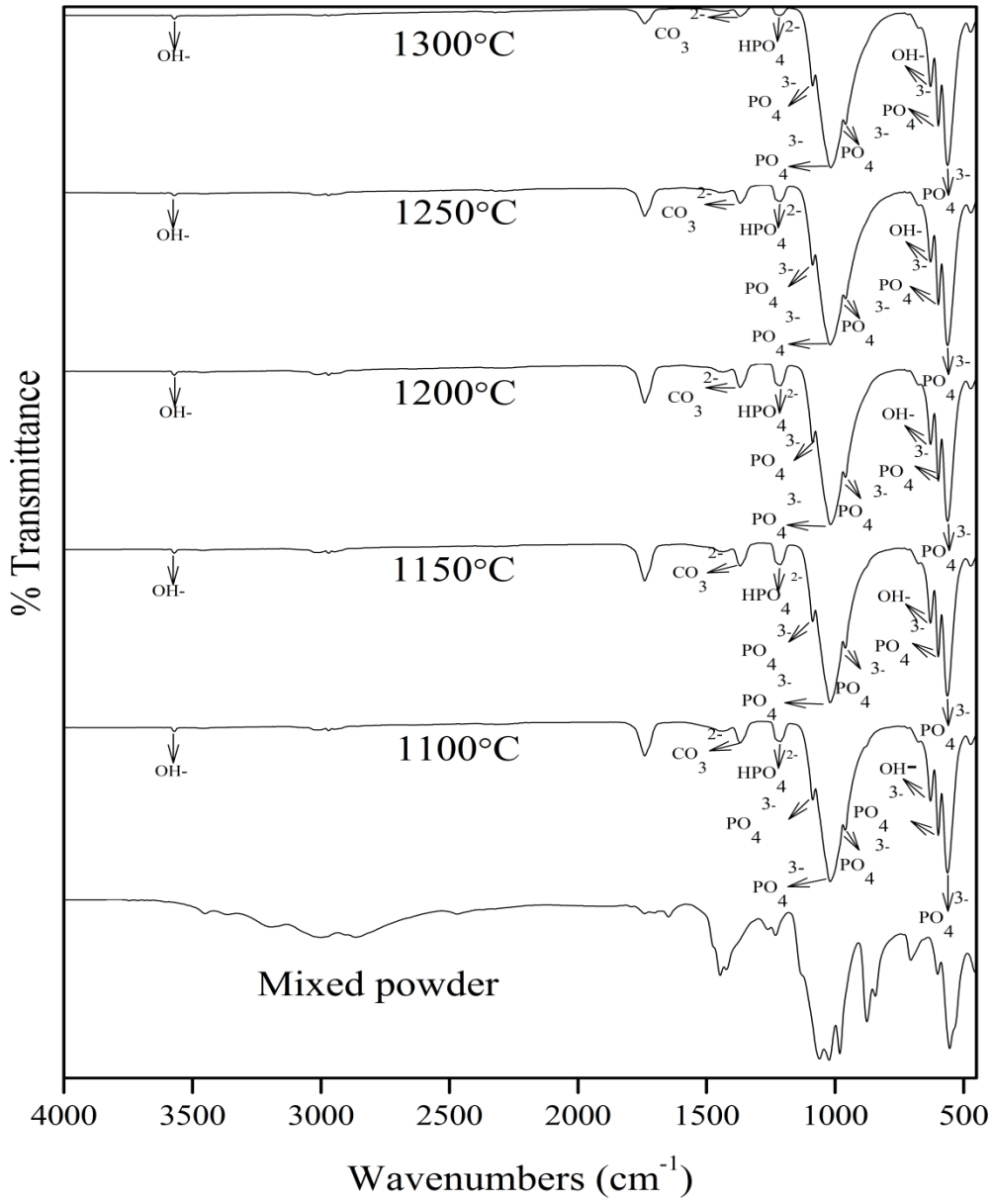


**Figure 25** FTIR spectra of mixed powder and sintered samples with ratio of 1.69 at 1100 °C (5A-2), 1150 °C (5B-2), 1200 °C (5C-2), 1250 (5D-2) and 1300 °C (5E-2) for 2 hours.

These samples were the optimize condition which, obtained from XRD and XRF data. The FTIR spectra of mixed powder revealed the broad band at around 2500-3700 $cm^{-1}$ corresponds to the absorbed hydrate of lattice $OH^-$ ions. Water molecules appear at 1647 $cm^{-1}$. The $HPO_4^{2-}$ ions are observed at 876 $cm^{-1}$ band, which exists in non-stoichiometric HA. The IR spectrum of sample ratio 1.69, sintered at 1100 ˚C for 2 hours was showed the bands corresponding to $PO_4^{3-}$ group at 1087, 1019, 960, 598 and 562 $cm^{-1}$, along with the bands at 3570 and 629 $cm^{-1}$ (librational mode) identified to $OH^-$ group. In addition, bands at 1369 $cm^{-1}$ can be observed, corresponding to vibration modes of carbonate group. The position of the carbonate band indicates that the $CO_3^{2-}$ groups were substituted the $PO_4^{3-}$ positions. The band of $HPO_4^{2-}$ at 1212 $cm^{-1}$ showed the formation of β-TCP which was phosphate group.

The IR spectrum of sample ratio 1.69, sintered at 1150 ˚C for 2 hours was showed the bands corresponding to $PO_4^{3-}$ group at 1087, 1019, 959, 598 and 563 $cm^{-1}$, along with the bands at 3570 and 629 $cm^{-1}$ (librational mode) identified to $OH^-$ group. In addition, bands at 1369 $cm^{-1}$ could be observed, corresponding to vibration modes of carbonate group. The position of the carbonate band indicated that the $CO_3^{2-}$ groups were substituted the $PO_4^{3-}$ positions. The band of $HPO_4^{2-}$ at 1212 $cm^{-1}$ showed the formation of β-TCP which is phosphate group.

The IR spectrum of sample with ratio 1.69, sintered at 1200 ˚C for 2 hours, was showed the bands corresponding to $PO_4^{3-}$ group at 1087, 1017, 959, 598 and 562 $cm^{-1}$, along with the bands at 3570 and 628 $cm^{-1}$ (librational mode) identified to $OH^-$ group. In addition, bands at 1369 $cm^{-1}$ could be observed, corresponding to vibration modes of carbonate group. The position of the carbonate band indicated that the $CO_3^{2-}$ groups were substituted the $PO_4^{3-}$ positions. The band of $HPO_4^{2-}$ at 1212 $cm^{-1}$ showed the formation of β-TCP which was phosphate group.

The IR spectrum of sample ratio 1.69, sintered at 1250 ˚C for 2 hours, was showed the bands corresponding to $PO_4^{3-}$ group at 1087, 1017, 958, 597 and 562 $cm^{-1}$, along with the bands at 3570 and 628 $cm^{-1}$ (librational mode) identified to $OH^-$ group. In addition, bands at 1369 $cm^{-1}$ could be observed, corresponding to vibration modes of carbonate group. The position of the carbonate band indicated that the $CO_3^{2-}$ groups

are substituted the $PO_4^{3-}$ positions. The band of $HPO_4^{2-}$ at 1212 $cm^{-1}$ showed the formation of β-TCP which was phosphate group.

The IR spectrum of sample ratio 1.69, sintered at 1300 ˚C for 2 hours, was showed the bands corresponding to $PO_4^{3-}$ group at 1087, 1019, 958, 597 and 562 $cm^{-1}$, along with the bands at 3570 and 628 $cm^{-1}$ (librational mode) identified to $OH^-$ group. In addition, bands at 1369 $cm^{-1}$ could be observed, corresponding to vibration modes of carbonate group. The position of the carbonate band indicated that the $CO_3^{2-}$ groups were substituted the $PO_4^{3-}$ positions. The band of $HPO_4^{2-}$ at 1212 $cm^{-1}$ showed the formation of β-TCP which was phosphate group.

In the FTIR spectra of powder sintered from 1100 to 1300 ˚C the bands identified to $PO_4^{3-}$, $OH^-$, $CO_3^{2-}$ and $HPO_4^{2-}$ groups was the same of all conditions. However, the difference of all samples was observed that the $CO_3^{2-}$ and $HPO_4^{2-}$ bands reduced in peak area at 1300 ˚C for 2 hours when compared with other condition. This study was in agreement with the characterization of XRD and chemical analysis. The results of characterization showed that all samples was a type B carbonate HA due to substituting a tetrahedral groups with $CO_3^{2-}$ groups and was calcium deficient HA due to substituted of $HPO_4^{2-}$ groups in the position of $PO_4^{3-}$ groups that characterized nonstoichiometric HA.

### 3.6 Microstructure characterization by SEM

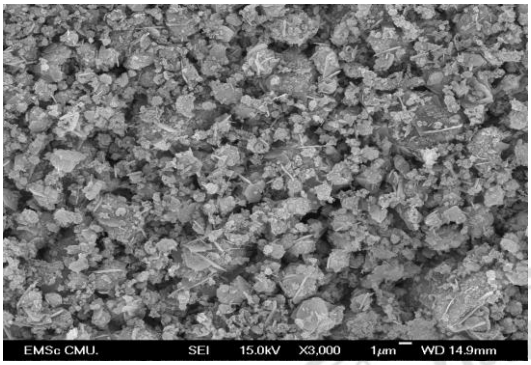


(a) Mixed powder

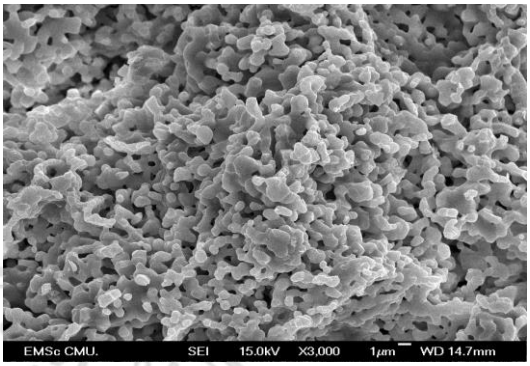


(b) 1100 °C

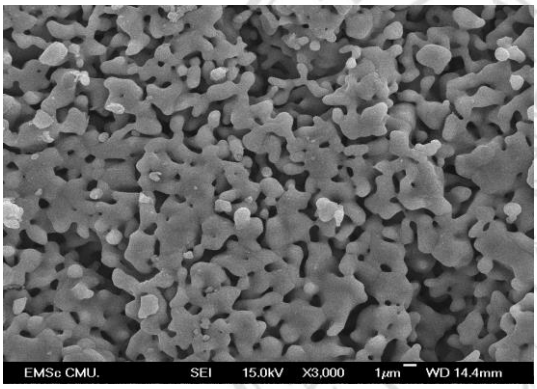


(c) 1150 °C

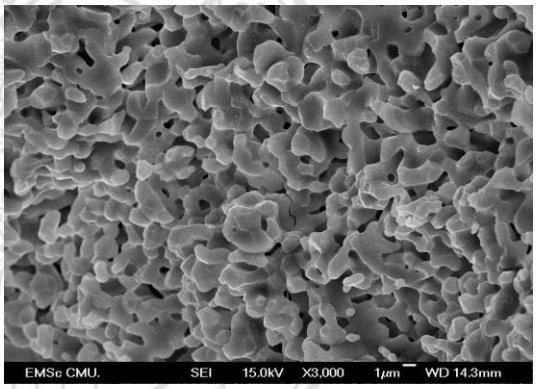


(d) 1200 °C

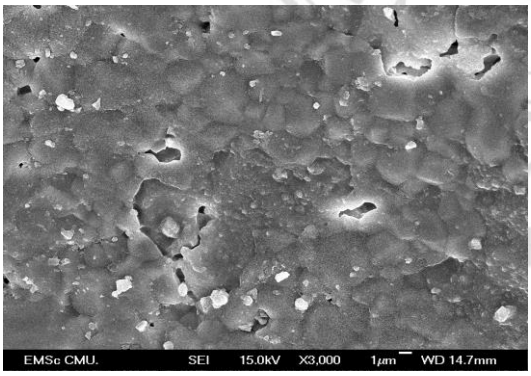


(e) 1250 °C

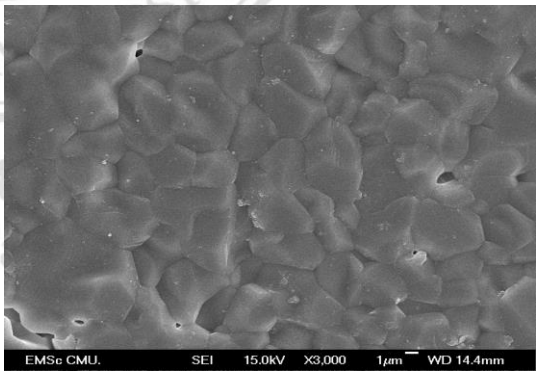


(f) 1300 °C

**Figure 26** SEM images of fracture surfaces of green body (a) and sintered sample with ratio 1.69 at various temperatures for 2 hours ((b) – (f)). (× 3,000)

The SEM showed fracture surface of green bodies in **Figure 26(a)**. The mixed powder consisted of mixtures of fine and hard particles. The hard particles were agglomerates and had the irregular shape. This figure was the optimized condition for synthesis HA of this research. The sample with ratio of 1.69 was sintered at 1100 to 1300 °C for 2 hours. **Figure 26(b)** showed fracture surface of sample with ratio of 1.69 at 1100 °C. It could be seen that grain size range from 0.5 to 1 μm. An apparent porosity had about 51 to 55 % of total area. The pore size range from 1 to 10 μm. **Figure 26(c)** showed the fracture surface of sample with ratio of 1.69 at 1150 °C. The increase of grain size had size range from 1 to 2 μm. An apparent porosity had about 50 % of total area. The pore size range from 1 to 4 μm. **Figure 26(d)** showed the fracture surface of sample with ratio of 1.69 at 1200 °C, and the increase of grain sizes was a range from 1.2 to 4 μm. An apparent porosity had about 45 to 50 % of total area. The total pore size range from 1 to 8 μm, while small pores had a size range from 1 to 2 μm and the bigger pore had a size range from 3 to 8 μm. This temperature showed the formation of closed pores. Some area of this figure showed the formation of the grain boundary crack. **Figure 26(e)** showed the fracture surface of sample with ratio of 1.69 at 1250 °C. There were more increase of grains size at 1200 °C and grain size in range of 2.5 to 4.5 μm. An apparent porosity had about 30 % of total area. The tiny pores had size less than 1 μm and observed on grain boundary. The opened pores showed the formation with size about 5 μm. **Figure 26(f)** showed the fracture surface of sample with ratio of 1.69 at 1300 °C. It could be seen grain growth clearly seen in this figure. The grain sizes were range from 3 to 8 μm. The formations of closed pores were observed that more than at 1250 °C. In **figure 26(f)** showed the image from SEM that could not be seen the crack between grain boundary but some of grain boundary remain the small pores which separated from the closed pores. Some area of this figure showed open pore that had sizes lower than 10 μm.

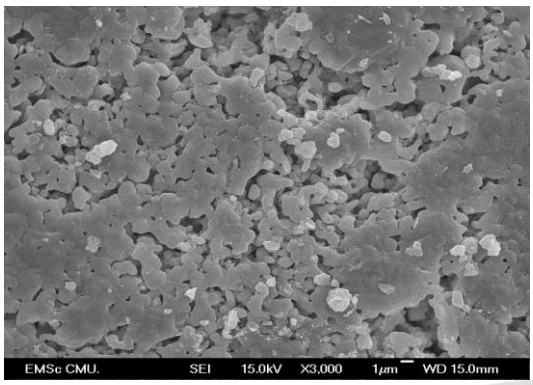


(a) 1100 °C

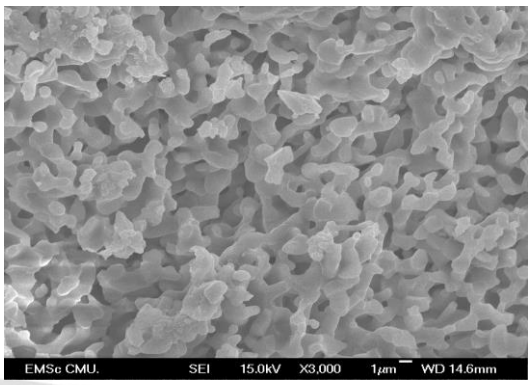


(b) 1150 °C

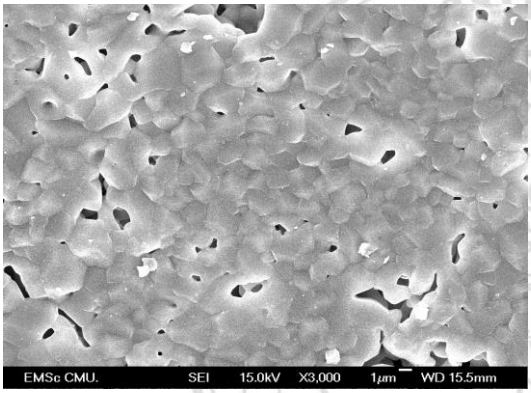


(c) 1200 °C

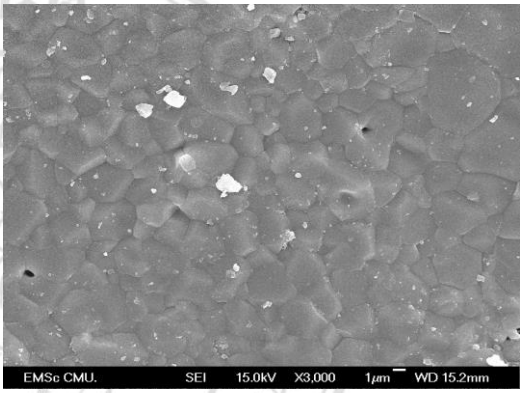


(d) 1250 °C

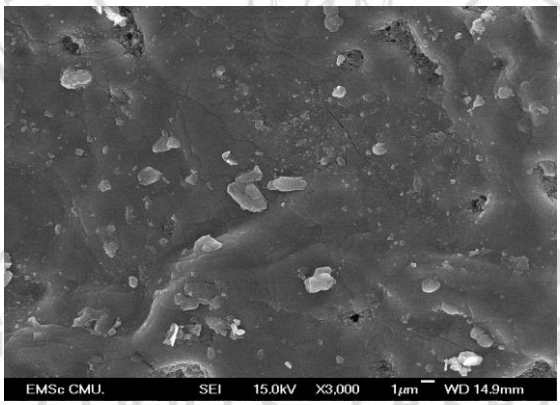


(e) 1300 °C

**Figure 27** SEM images of fracture surfaces of sintered sample with ratio 1.69 at various temperatures for 5 hours. (x3,000)

The sample with ratio of 1.69 was sintered at temperatures range from 1100 to 1300 °C for 5 hours. **Figure 27(a)** showed the fracture surface of sample at 1100 °C which grain size in the range of 1 to 1.3 μm. An apparent porosity had higher than 50 % of total area. The average pore size range from 1 to 10 μm. **Figure 27(b)** showed the fracture surface of sample at 1150 °C. The increase of grain size had size range from 1.2 to 4 μm. An apparent porosity had about 50 to 52 % of total area. The pore size range from 1 to 8 μm. **Figure 27(c)** showed the fracture surface of samples at 1200 °C, and the increased of grain size was a range from 1.5 to 5 μm. An apparent porosity had about 47 to 50 % of total area. **Figure 27(d)** showed the fracture surface of sample at 1250 °C. An average grain size was range from 2 to 7 μm. An apparent porosity had about 30 % of total area. The tiny pores which had size less than 1 μm were observed on grain boundary, and some opened pores showed the formation of pore size higher than 1 μm. **Figure 27(e)** showed the fracture surface of sample at 1300 °C. An abnormal of grain growth was clearly seen in this figure. The grain size was range from 6 to 12 μm. This phenomenon had been on surface of grain and grain boundary at this temperature which seen the crack on grain and crack internal grain.

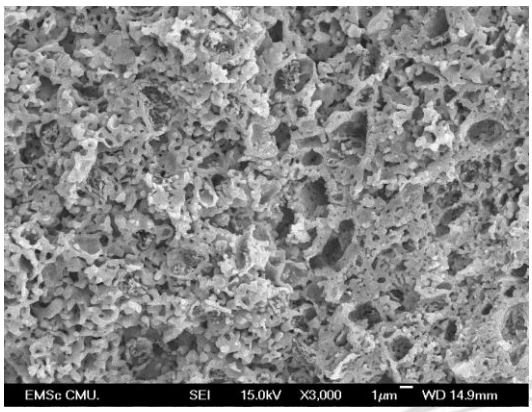


(a) 1100 °C

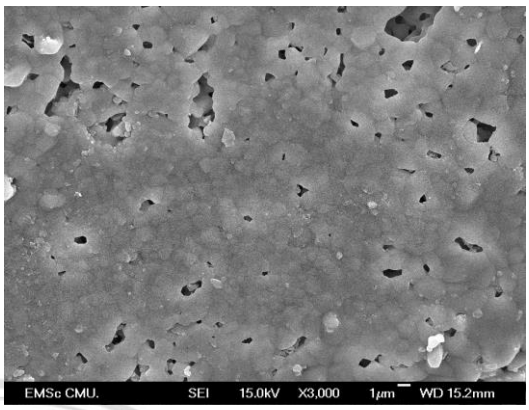


(b) 1150 °C

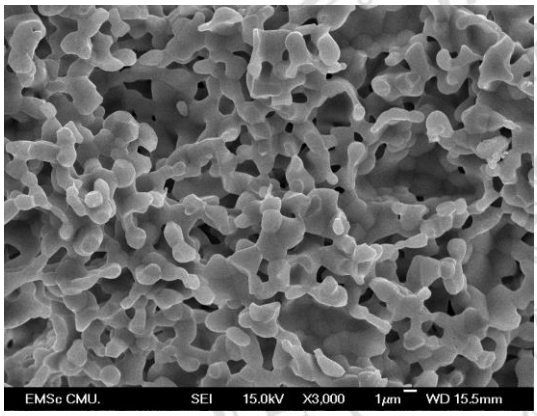


(c) 1200 °C

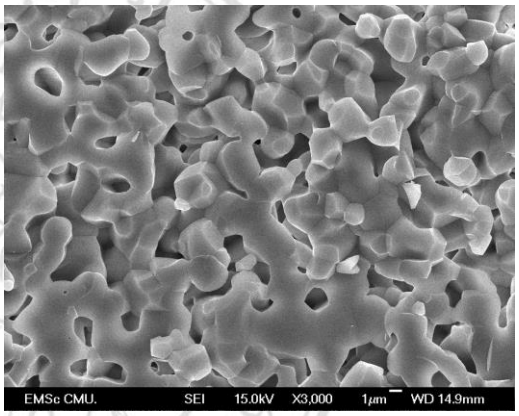


(d) 1250 °C

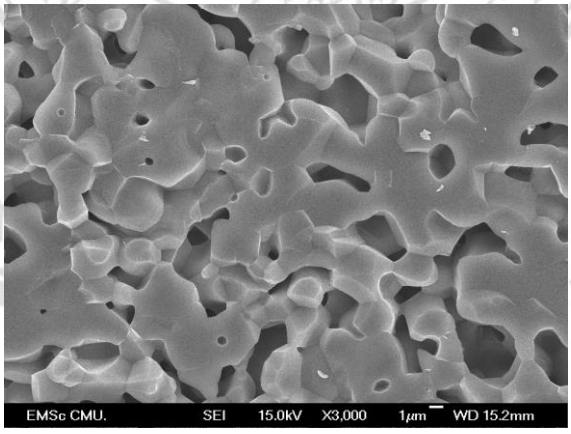


(e) 1300 °C

**Figure 28** SEM images of surface fracture of sintered sample with ratio of 1.65 at various temperatures for 2 hours. (x3,000)

The sample with ratio of 1.65 was sintered at temperatures range from 1100 to 1300 °C for 2 hours. **Figure 28(a)** showed the fracture surface of 1.65 samples at 1100 °C. It could be seen that grain size was 1 μm. An apparent porosity had about 54 to 57% of total area. **Figure 28(b)** showed the fracture surface of sample ratio of 1.65 at 1150 °C. The increase of grain size had range from 1 to 1.5 μm. An apparent porosity had about 56 % of total area. An average pore size range from 1 to 6 μm. **Figure 28(c)** showed the fracture surface of sample at 1200 °C. This figure showed the increase of grains size was a range from 1.2 to 3 μm. An apparent porosity had about 50 % of total area. The pore size range from 1 to 10 μm. **Figure 28(d)** showed the fracture surface of sample at 1250 °C. The grain size was range 1.3 to 5.2 μm. An apparent porosity had about 50 % of total area. This figure showed that opened pores and closed pores remained in the microstructure. This phenomenon had effected on the density and mechanical properties due to amounts of β-TCP had excess. **Figure 28(e)** showed the fracture surface of sample at 1300 °C. Grain growth was clearly seen in this figure. The grain size was range 3 to 7 μm but an apparent porosity had about 50 % of total area. When compared to the sample with ratio of 1.69 at 1300 for 2 hours, apparent porosity had much difference between two conditions in the same temperature.

### 3.7 Mechanical properties of sintered samples.

3.7.1 Hardness

**Table 8** Results of hardness value (HV) of all sintered samples

| Sintering condition | | Ca/P | | | | |
|---|---|---|---|---|---|---|
| | | 1.65 | 1.66 | 1.67 | 1.68 | 1.69 |
| 2 h | 1100°C | 4.58 ± 0.58 | 4.91 ± 0.54 | 5.98 ± 0.80 | 6.16 ± 0.79 | 7.48 ± 1.05 |
| | 1150°C | 4.78 ± 0.56 | 5.27 ± 0.31 | 6.36 ± 0.62 | 8.52 ± 0.57 | 9.13 ± 0.85 |
| | 1200°C | 12.97 ± 0.34 | 13.38 ± 0.81 | 14.13 ± 2.36 | 14.56 ± 1.34 | 19.20 ± 3.19 |
| | 1250°C | 13.96 ± 1.09 | 18.58 ± 0.50 | 18.87 ± 0.46 | 22.58 ± 0.81 | 34.73 ± 3.89 |
| | 1300°C | 14.25 ± 0.28 | 18.98 ± 0.54 | 28.60 ± 1.78 | 37.55 ± 4.30 | 39.80 ± 4.78 |
| 3 h | 1100°C | 6.96 ± 1.01 | 7.28 ± 0.97 | 7.98 ± 1.07 | 8.38 ± 0.44 | 8.88 ± 0.42 |
| | 1150°C | 9.43 ± 0.90 | 11.34 ± 0.50 | 12.90 ± 0.31 | 12.98 ± 0.33 | 13.75 ± 0.43 |
| | 1200°C | 9.85 ± 0.82 | 11.56 ± 0.51 | 13.33 ± 0.22 | 14.88 ± 0.68 | 18.86 ± 0.58 |
| | 1250°C | 18.66 ± 0.37 | 22.78 ± 0.87 | 29.04 ± 1.14 | 29.90 ± 2.31 | 30.02 ± 1.61 |
| | 1300°C | 17.37 ± 1.75 | 20.20 ± 1.81 | 22.92 ± 0.89 | 24.38 ± 0.94 | 28.64 ± 1.82 |
| 4 h | 1100°C | 5.05 ± 0.14 | 5.38 ± 0.38 | 8.18 ± 0.57 | 8.80 ± 0.54 | 10.18 ± 0.81 |
| | 1150°C | 8.64 ± 0.45 | 9.00 ± 0.32 | 12.75 ± 0.30 | 13.65 ± 0.62 | 18.45 ± 0.37 |
| | 1200°C | 10.38 ± 0.58 | 13.68 ± 0.86 | 13.84 ± 1.07 | 18.48 ± 1.28 | 19.25 ± 1.47 |
| | 1250°C | 18.78 ± 0.45 | 19.92 ± 1.55 | 30.56 ± 1.81 | 32.94 ± 2.92 | 33.45 ± 3.66 |
| | 1300°C | 14.44 ± 1.07 | 19.34 ± 0.63 | 24.22 ± 0.93 | 24.92 ± 1.06 | 29.42 ± 1.29 |
| 5 h | 1100°C | 4.73 ± 0.28 | 4.87 ± 0.23 | 5.70 ± 0.92 | 8.72 ± 0.61 | 10.90 ± 0.44 |
| | 1150°C | 8.32 ± 0.48 | 9.00 ± 0.32 | 11.28 ± 0.44 | 13.12 ± 0.80 | 14.38 ± 0.58 |
| | 1200°C | 12.00 ± 0.45 | 13.20 ± 0.27 | 14.22 ± 1.12 | 15.24 ± 0.69 | 20.25 ± 1.58 |
| | 1250°C | 19.08 ± 0.52 | 19.92 ± 1.70 | 32.47 ± 1.57 | 33.67 ± 3.51 | 36.40 ± 3.57 |
| | 1300°C | 19.56 ± 0.57 | 20.88 ± 1.98 | 23.56 ± 1.01 | 25.43 ± 0.78 | 34.16 ± 3.12 |

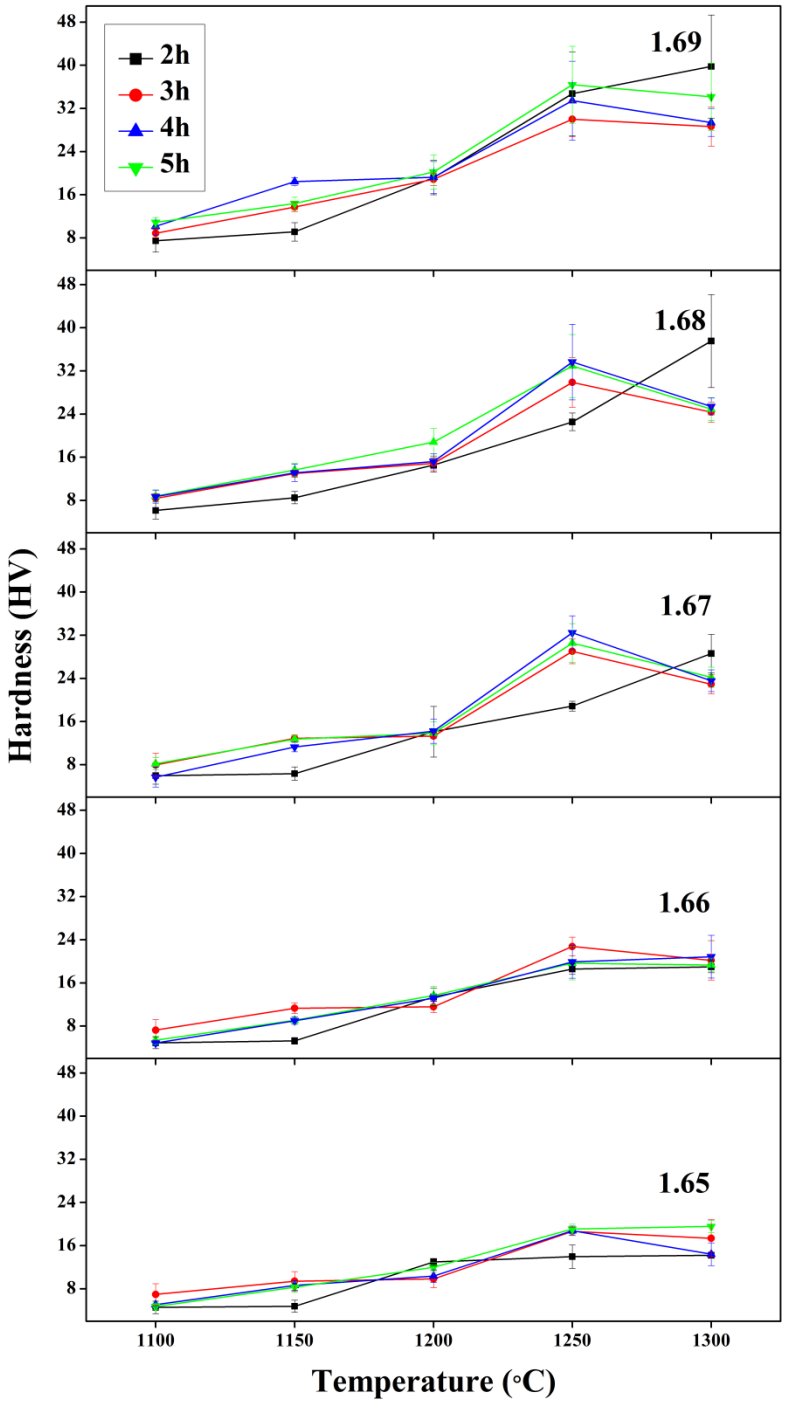


**Figure 29** Hardness of sample ratios 1.65, 1.66, 1.67, 1.68 and 1.69 at different temperatures and soaking times.

**Figure 29** showed the influence of sintering temperatures and soaking times on hardness of samples with ratios 1.65 to 1.69 at various temperatures from 1100 °C to 1300 °C for 2 to 5 hours. Hardness of the samples with ratio of 1.65 and 1.66 were observed after sintering at 1100 °C, and it had trend to increase, followed by the increase of the temperature at 1300 °C for 2 and 5 hours, but for 3 and 4 hours, hardness had trend to increase at 1250 °C and decrease at 1300 °C due to the existence of closed pores, grains growth or coalescence and point defects. Hardness of the samples with ratio of 1.67, 1.68 and 1.69 were observed after sintering at 1100 °C, and it had trend to increase, followed by the increase of the temperature at 1300 °C for 2 hours, but for 3, 4 and 5 hours, hardness had trend to increase at 1250 °C and decrease at 1300 °C. The maximum value of hardness of sample groups with ratio of 1.65 was 19.56 ± 0.57 HV at 1300 °C for 5 hours. The maximum value of hardness of sample groups with ratio of 1.66 was 22.78 ± 0.87 HV at 1250 °C for 3 hours. The maximum value of hardness of sample groups with ratio of 1.67 was 32.47 ± 1.57 HV at 1250 °C for 5 hours. The maximum value of hardness of sample groups with ratio of 1.68 was 37.55 ± 4.30 HV at 1300 °C for 2 hours. The maximum value of hardness of sample groups with ratio of 1.69 was 39.88 ± 4.78 HV at 1300 °C for 2 hours. This group was the optimized condition of the experimental due to highest when compared with other condition. However, it had hardness lower than theoretical hardness of pure HA (600 HV) due to affected of highly porous and point defect ($OH^-$, $PO_4^{3-}$ and $Ca^{2+}$) of samples. These curves revealed a significant loss in hardness at 1300 °C which related with the apparent and bulk density change affected on sintering. These data were clearly exhibit that the maximum hardness corresponds to the maximum of density.

3.7.2 Flexural bending strength

**Table 9** Results of flexural bending strength value (MPa) of all sintered samples

| Sintering condition | | Ca/P | | | | |
|---|---|---|---|---|---|---|
| | | 1.65 | 1.66 | 1.67 | 1.68 | 1.69 |
| 2 h | 1100°C | 1.43 ± 0.18 | 1.78 ± 0.08 | 2.45 ± 0.25 | 2.48 ± 0.06 | 2.60 ± 0.26 |
| | 1150°C | 1.50 ± 0.19 | 1.96 ± 0.09 | 2.49 ± 0.06 | 2.74 ± 0.15 | 2.97 ± 0.15 |
| | 1200°C | 3.59 ± 0.19 | 3.84 ± 0.17 | 4.24 ± 0.18 | 4.37 ± 0.18 | 5.96 ± 0.12 |
| | 1250°C | 4.23 ± 0.18 | 5.27 ± 0.18 | 7.75 ± 0.71 | 7.11 ± 0.83 | 13.60 ± 0.69 |
| | 1300°C | 4.28 ± 0.18 | 5.93 ± 0.31 | 5.90 ± 0.12 | 12.96 ± 0.78 | 12.00 ± 0.54 |
| 3 h | 1100°C | 2.51 ± 0.06 | 2.55 ± 0.08 | 2.62 ± 0.10 | 2.72 ± 0.27 | 2.86 ± 0.21 |
| | 1150°C | 2.98 ± 0.22 | 3.21 ± 0.07 | 3.54 ± 0.13 | 3.64 ± 0.20 | 3.95 ± 0.10 |
| | 1200°C | 2.99 ± 0.22 | 3.22 ± 0.07 | 3.79 ± 0.20 | 4.37 ± 0.20 | 5.66 ± 0.19 |
| | 1250°C | 5.07 ± 0.17 | 6.83 ± 0.13 | 7.20 ± 0.34 | 7.43 ± 0.16 | 8.01 ± 0.60 |
| | 1300°C | 5.29 ± 0.28 | 7.14 ± 0.84 | 8.06 ± 0.60 | 8.95 ± 0.89 | 9.07 ± 0.51 |
| 4 h | 1100°C | 1.90 ± 0.08 | 1.99 ± 0.09 | 2.70 ± 0.09 | 2.81 ± 0.19 | 3.00 ± 0.15 |
| | 1150°C | 2.76 ± 0.11 | 2.96 ± 0.22 | 3.46 ± 0.13 | 3.87 ± 0.09 | 5.16 ± 0.27 |
| | 1200°C | 3.03 ± 0.37 | 3.89 ± 0.09 | 3.96 ± 0.10 | 5.18 ± 0.27 | 6.05 ± 0.12 |
| | 1250°C | 4.34 ± 0.20 | 6.09 ± 0.27 | 7.31 ± 0.34 | 7.59 ± 0.28 | 8.21 ± 0.61 |
| | 1300°C | 5.32 ± 0.11 | 6.20 ± 0.27 | 9.64 ± 0.22 | 10.98 ± 0.67 | 11.07 ± 0.67 |
| 5 h | 1100°C | 1.47 ± 0.18 | 1.51 ± 0.19 | 2.35 ± 0.06 | 2.79 ± 0.14 | 3.12 ± 0.22 |
| | 1150°C | 2.71 ± 0.11 | 2.88 ± 0.11 | 3.17 ± 0.07 | 3.70 ± 0.14 | 4.32 ± 0.20 |
| | 1200°C | 3.31 ± 0.07 | 3.77 ± 0.14 | 4.27 ± 0.15 | 4.97 ± 0.17 | 6.93 ± 0.81 |
| | 1250°C | 5.93 ± 0.12 | 6.63 ± 0.27 | 7.23 ± 0.34 | 7.74 ± 0.58 | 11.99 ± 0.54 |
| | 1300°C | 6.19 ± 0.27 | 7.06 ± 0.83 | 9.96 ± 0.08 | 11.79 ± 0.91 | 12.11 ± 0.54 |

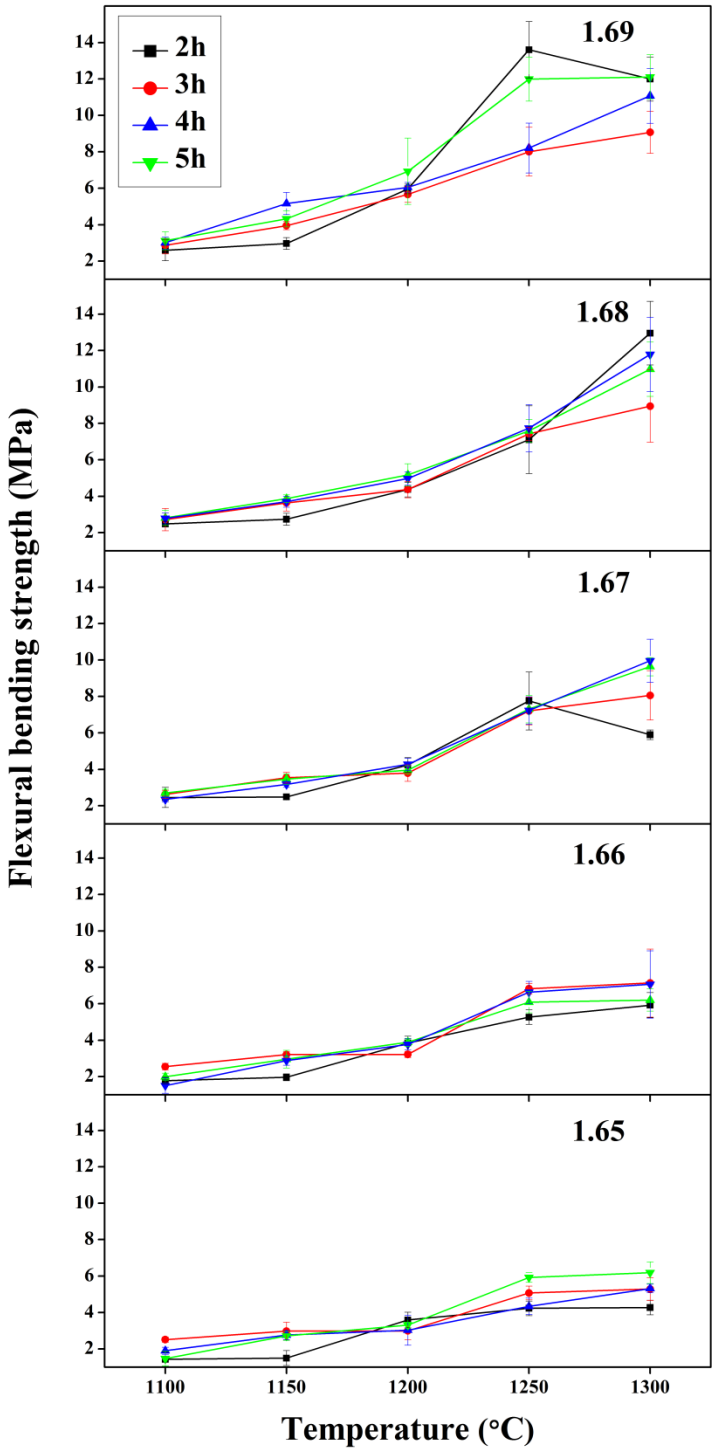


**Figure 30** Flexural bending strength of sample ratios 1.65, 1.66, 1.67, 1.68 and 1.69 at different temperatures and times.

**Figure 30** showed the variation of the bending strength, temperatures and times of samples with ratio of 1.65 to 1.69. The bending strength of the samples with ratio of 1.65, 1.66 and 1.68 were observed after sintering at 1100 °C, and it had trend to increase, followed by the increase of the temperature at 1300 °C for 2 to 5 hours. The bending strength of sample with ratio of 1.67 and 1.69 were observed after sintering at 1100 °C, and it had trend to increase at 1250 °C and to decrease at 1300 °C for 2 hours, while the bending strength for 3, 4 and 5 hours were increased to maximum value at 1300 °C. This could explain the phenomenon obtained from pore growth or pore became larger normal and caused by affected of CaO and β-TCP lead to internal stresses and cracking at grain boundaries of samples at 1300 °C and increasing of strength related with decreasing of close pores and increase of the finer grain sizes at high temperature. However, there were tendencies of lower strength when grain growth and porosity increased at higher temperature (above 1250 °C). The maximum value of bending strength of sample groups with ratio of 1.65 was 6.19 ± 0.27 MPa at 1300 °C for 5 hours. The maximum value of bending strength of sample groups with ratio of 1.66 was 7.14 ± 0.84 MPa at 1300 °C for 3 hours. The maximum value of bending strength of sample groups with ratio of 1.67 was 9.96 ± 0.08 MPa at 1300 °C for 5 hours. The maximum value of bending strength of sample groups with ratio of 1.68 was 12.96 ± 0.78 MPa at 1300 °C for 2 hours. The maximum value of bending strength of sample groups with ratio of 1.69 was 13.60 ± 0.69 MPa at 1250 °C for 2 hours. This group was the optimized condition of the experimental due to highest when compared with other condition. However, it had bending strength lower than theoretical bending strength of pure HA (115-200 MPa), but it was in range of cancellous bone (10-20 MPa).

### 3.8 Biological characterization

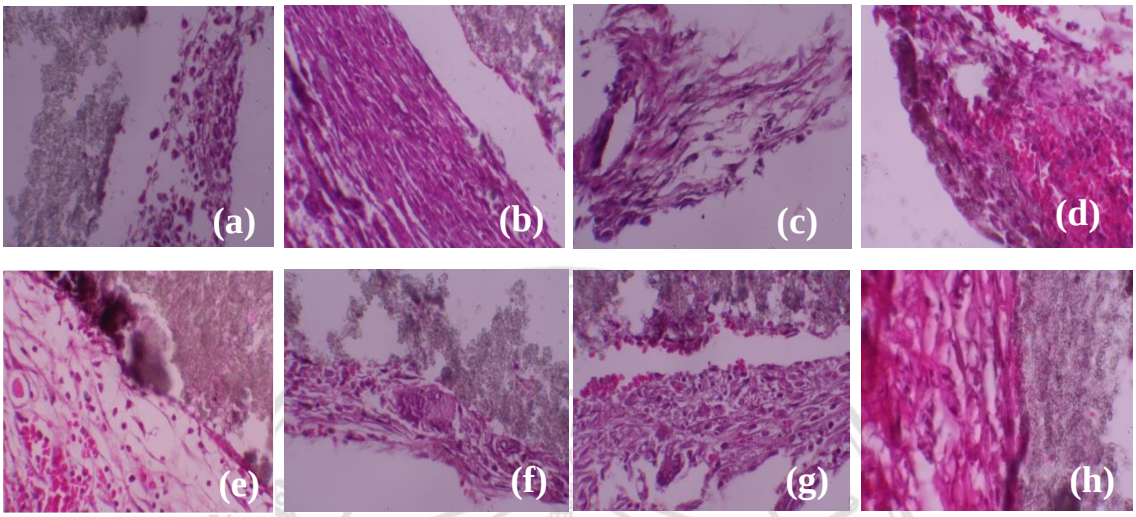


**Figure 31** Histological images of sample with ratio of 1.69 in soft tissue; (a) 3 days, (b) 7 days, (c) 14 days, (d) 21 days, (e) 30 days, (f) 45 days, (g) 90 days, (h) 180 days

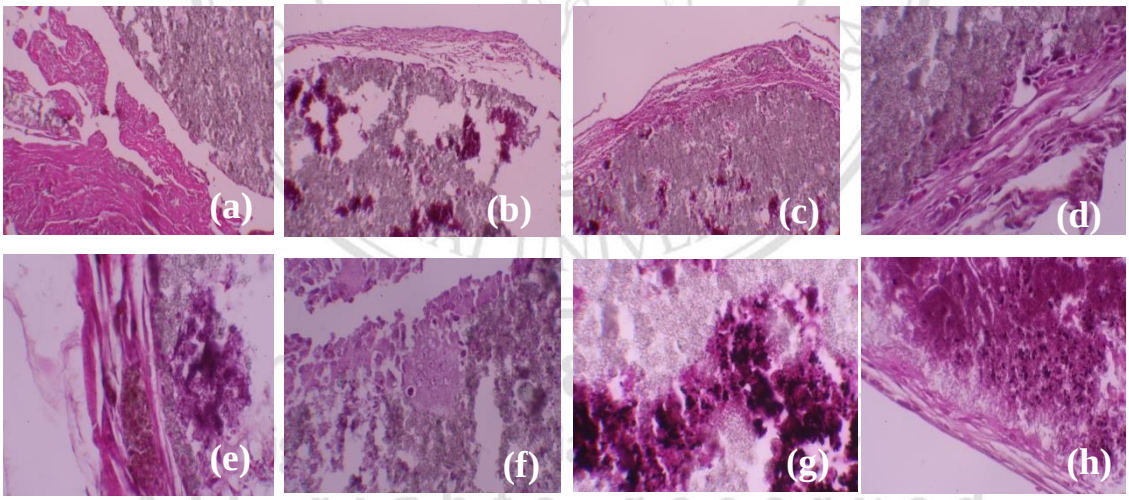


**Figure 32** Histological images of sample with ratio of 1.65 in soft tissue; (a) 3 days, (b) 7 days, (c) 14 days, (d) 21 days, (e) 30 days, (f) 45 days, (g) 90 days, (h) 180 days

**Table 10** Results of foreign body reaction on soft tissue response after implantation for sample bodies with ratios 1.69 and 1.65 at 1300 °C for 2 hours.

| Tissue reaction | Ca/P mole ratios | Time periods (days) | | | | | | | |
|---|---|---|---|---|---|---|---|---|---|
| | | 3 | 7 | 14 | 21 | 30 | 45 | 90 | 180 |
| Reaction grading | 1.69 | ♦ | ♦♦ | ♦♦ | ♦♦ | ♦ | ♦♦ | ♦ | ♦ |
| | 1.65 | ♦ | ♦ | ♦♦ | ♦♦ | ♦♦ | ♦♦♦ | ♦♦♦ | ♦♦ |
| Cellular infiltration into ceramic body | 1.69 | ⊗ | ⊗ | ⊗ | ⊗ | ⊗ | √ | ⊗ | ⊗ |
| | 1.65 | ⊗ | √ | √ | √ | √ | √ | √ | √ |
| Calcification in ceramic body | 1.69 | ⊗ | ⊗ | ⊗ | ⊗ | √ | √ | √ | √ |
| | 1.65 | √ | √ | √ | √ | √ | √ | √ | √ |
| Displacement of ceramic components into surrounding host tissue | 1.69 | √ | √ | ⊗ | √ | √ | √ | ⊗ | ⊗ |
| | 1.65 | √ | √ | √ | √ | √ | √ | √ | √ |

**Note:** Symbol ♦ = mild reaction, ♦♦ = moderate reaction and ♦♦♦ = severe reaction

Symbol ⊗ = absent and √ = present

Microscopic description of the sections presented fragments of the samples with ratio of 1.69 with walling off fibro adipose tissue. At 3 days after implantation, those with ratio of 1.69 had mild foreign body reaction, while those with 1.65 had mild foreign body reaction. Moreover, a cellular infiltration into the bodies of sample with ratio 1.69 and 1.65 was absent. Furthermore, dystrophic calcification in the bulk sample with ratio of 1.69 and 1.65 was absent and present, respectively. This difference was caused by the fact that the quantity of CaO phase was higher in the samples with ratio 1.65 than those with ratio 1.69 according to XRD data. Besides, the degradation of body components of the samples with ratio of 1.69 and 1.65 into

surrounding host tissues was presented in both due to high solubility of β-TCP into the ceramic body (**Figure 31(a) and 32 (a**)).

At 7 days, an inflammatory response of the samples ratio of 1.69 and 1.65 was moderate and mild foreign body reaction respectively. The samples with ratio of 1.69 showed the increase of inflammatory cells, but the samples with ratio of 1.65 showed the constant of inflammatory cells in bodies. Apart from that, a cellular infiltration into the bodies of the samples with ratio of 1.69 and 1.65 was absent and present respectively because to the sample with ratio 1.69 had lower porosity than the sample with ratio 1.65. Further, dystrophic calcification in the bulk samples with ratio of 1.69 and 1.65 was absent and present respectively. This difference was caused by the fact that the quantity of CaO phase was higher in the samples with ratio 1.65 than those with ratio 1.69. Besides, the degradation of body components of the samples with ratio of 1.69 and 1.65 into surrounding host tissue was presented in both (**Figure 31(b) and 32(b)**).

At 14 days, an inflammatory response of the samples ratio of 1.69 and 1.65 was moderate foreign body reaction. The samples with ratio of 1.69 showed the constant of inflammatory cells, but the samples with ratio of 1.65 showed the increase of inflammatory cells in bodies. This phenomenon may be caused by high quantity of β-TCP phase in the sample with ratio of 1.65 which affected high solubility of the samples. Apart from that, a cellular infiltration into the bodies of samples with ratio of 1.69 and 1.65 was absent and present respectively which result was same at 7 days. Dystrophic calcification in the bulk samples with ratio of 1.69 and 1.65 was constant. Finally, the degradation of body components of the samples with ratio of 1.69 and 1.65 was absent and present respectively (**Figure 31(c) and 32(c)**).

At 21 days, an inflammatory response of the samples ratio of 1.69 and 1.65 was moderate foreign body reaction. The samples with ratio of 1.69 and 1.65 showed inflammatory were constant. A cellular infiltration into the bodies of samples with ratio of 1.69 and 1.65 was same at 14 days. Further, dystrophic calcification in the bulk samples with ratio of 1.69 and 1.65 was constant.

Finally, the degradation of body components of the samples with ratio of 1.69 and 1.65 was present. This result showed that samples with ratio of 1.69 had β-TCP which soluble from bodies (**Figure 31(d) and 32(d)**).

At 30 days, an inflammatory response of the samples ratio of 1.69 and 1.65 was mild and moderate foreign body reaction respectively. The samples with ratio of 1.69 showed the decrease of inflammatory cells, but the samples with ratio of 1.65 showed were constant of in bodies. Apart from that, a cellular infiltration into the bodies of the samples with ratio of 1.69 and 1.65 was absent and present respectively because to the sample with ratio 1.69 had lower porosity than the sample with ratio 1.65. Further, dystrophic calcification in the bulk samples with ratio of 1.69 and 1.65 was present in both because CaO phase still remained in bodies of both samples. Finally, the degradation of body components of the samples with ratio of 1.69 and 1.65 into surrounding host tissues was present in both due to high solubility of β-TCP into the bodies (**Figure 31(e) and 32(e)**).

At 45 days, an inflammatory response of the samples ratio of 1.69 and 1.65 was moderate and severe foreign body reaction respectively. The samples with ratio of 1.69 showed the increase of inflammatory cells, while the samples with ratio of 1.65 showed the increase of inflammatory cells in bodies. Apart from that, a cellular infiltration into the bodies of the samples with ratio of 1.69 and 1.65 was present in both. Further, dystrophic calcification in the bulk samples with ratio of 1.69 and 1.65 was present in both. Finally, the degradation of body components of the samples with ratio of 1.69 and 1.65 into surrounding host tissues was present in both (**Figure 31(f) and 32(f)**).



At 90 days, an inflammatory response of the samples ratio of 1.69 and 1.65 was mild and severe foreign body reaction respectively. The samples with ratio of 1.69 showed the decrease of, but the samples with ratio of 1.65 showed inflammatory cells were constant. This phenomenon may be caused by high quantity of β-TCP phase in the sample with ratio of 1.65 which affected high solubility of the samples too. What's more, a cellular infiltration into the bodies of the samples with ratio of 1.69 and 1.65 was absent and present respectively due to the difference of porosity.

Moreover, dystrophic calcification in the bulk samples with ratio of 1.69 and 1.65 was present in both due to CaO phase still remained in bodies of both samples. However, small areas of calcification into the samples with ratio of 1.69 were found, while large areas of calcification into the samples with ratio 1.65 were observed. Besides, the degradation of body components of the samples with ratio of 1.69 and 1.65 into surrounding host tissues was absent and present respectively. This difference may be caused by the fact that the samples with ratio of 1.69 started becoming stable in an animal body, but the samples with ratio of 1.65 was not stable due to continuously dissolution of ceramic components (**Figure 31(g) and 32(g)**).

At 180 days, an inflammatory response of the samples ratio of 1.69 and 1.65 was mild and moderate foreign body reaction respectively. The samples with ratio of 1.69 showed inflammatory cells were constant, but the samples with ratio of 1.65 showed the decrease of inflammatory cells in bodies. What's more, a cellular infiltration into the bodies of the samples with ratio of 1.69 and 1.65 was absent and present respectively. Moreover, dystrophic calcification in the bulk samples with ratio of 1.69 and 1.65 was present in both of samples. Besides, the degradation of body components of the samples with ratio of 1.69 and 1.65 into surrounding host tissues was absent and present respectively. This result may be caused by the fact that the samples with ratio of 1.69 was stable in an animal body, but the samples with ratio of 1.65 was not stable due to continuously dissolution of ceramic components (**Figure 31(h) and 32(h)**).

**Table 10** revealed the overall picture throughout the time periods from 3 days to 180 days. The samples with Ca/P ratio of 1.69 had inflammation lower than those with Ca/P ratio of 1.65. This result indicated that the samples with ratio of 1.69 which had higher content of HA than those with ratio of 1.65. Therefore, the former had higher stability than the latter, and the former was non-resorbable material due to lower β-TCP while the latter was resorbable due to higher β-TCP. The apparent porosity of the samples with ratio of 1.65 was 51.2 % which was porous material, while the samples with ratio of 1.69 were 24.37 % which was rather dense material.

The apparent porosity was an important parameter that supported infiltration of cells into the samples bodies. SEM analysis of the samples with ratio of 1.69 revealed that pore size range from 1 to 10 μm, but infiltration of the cells into the body did not occur. The calcification was another factor that prevented cells from infiltrating into the sample bodies with ratio 1.69 because CaO phase in microstructure still remained.